Astronomy & Astrophysics manuscript no. output
July 29, 2022
©ESO 2022

Short period pulsating hot subdwarf stars observed by TESS

I. Southern Ecliptic Hemisphere

A.S. Baran[1,2,3], V. Van Grootel[4], R.H. Østensen[3,5], S.K. Sahoo[1,6], H.L. Worters[7], S.Sanjayan[1,6], S. Charpinet[8], P. Nemeth[9,10], J.H. Telting[11,12], D. Kilkenny[13]

[1] ARDASTELLA Research Group
[2] TBA
[3] Department of Physics, Astronomy, and Materials Science, Missouri State University, Springfield, MO 65897, USA
[4] Space sciences, Technologies and Astrophysics Research (STAR) Institute, Université de Liège, 19C Allée du 6 Août, B-4000 Liège, Belgium
[5] Recogito AS, Storgaten 72, N-8200 Fauske, Norway
[6] Nicolaus Copernicus Astronomical Centre of the Polish Academy of Sciences, ul. Bartycka 18, 00-716 Warsaw, Poland
[7] South African Astronomical Observatory, Observatory 7935, South Africa
[8] IRAP, CNRS, UPS, CNES, Université de Toulouse, Toulouse, France
[9] Astronomical Institute of the Czech Academy of Sciences, Fričova 298, CZ-251 65 Ondřejov, Czech Republic
[10] Astroserver.org, Fő tér 1, 8533 Malomsok, Hungary
[11] Nordic Optical Telescope, Rambla José Ana Fernández Pérez 7, 38711 Breña Baja, Spain
[12] Department of Physics and Astronomy, Aarhus University, NyMunkegade 120, DK-8000 Aarhus C, Denmark
[13] Department of Physics and Astronomy, University of the Western Cape, Private Bag X17, Bellville 7535, South Africa

ABSTRACT

We present results of a survey to search for short period pulsations in compact stellar objects during Year 1 and 3 of the *TESS* mission. The Southern Ecliptic Hemisphere has been observed. We described the *TESS* data used and the details of the search method. For the new detections we used unpublished spectroscopic observations to separate the objects into accurate classes. From the *TESS* photometry we clearly identify 41 short period hot subdwarf pulsators out of which eight show signals at both low and high frequencies. We report the list of prewhitened frequencies and we show the amplitude spectra calculated from the *TESS* data. We make an attempt to identify possible multiplets caused by stellar rotation and we select a few candidates translating to rotation period between 0.7 and 12.9 d. The most interesting targets discovered in this survey should be observed throughout the remainder of the *TESS* mission and from the ground. Asteroseismic investigations of these data sets will be invaluable in revealing the interior structure of these stars and will boost our understanding of their evolutionary history. We find three additional new variable stars but their spectral and variability types remain unknown.

Key words. Stars: oscillations - Asteroseismology - Stars: variable stars

1. Introduction

Hot subdwarf stars are evolved objects coming with O, OB and B spectral types, and a selection of variable H and He content in their atmospheres. The subdwarf B (sdB) stars have a surface effective temperature $T_{\rm eff}$ between 20 000 and 40 000 K, the logarithm of surface gravity $\log(g/{\rm cm\,s^{-2}})$ between 5 and 6, and a surface helium abundance usually strongly depleted compared to solar. The surface distribution of elements heavier than helium differs significantly from star to star (Geier 2013). The sdB stars are located on the blue extension of the horizontal branch (EHB) and are core-He burning stars, of about a half solar mass (Fontaine et al. 2012). The progenitors of hot subdwarfs are intermediate-mass stars ($\sim 1-3 M_{\odot}$) that must have lost significant mass during the red-giant branch, leaving them with only a tiny remnant of their hydrogen envelopes. The mass loss must happen before helium ignition, otherwise they would become He-core low-mass white dwarfs (without He-core burning), or normal horizontal branch stars (He-core burning, but with a much lower effective temperature, thicker H-rich envelopes and higher masses). Binary population synthesis modeling has been performed exploring various mass-loss scenarios, as detailed by Han et al. (2002).

Hot subdwarfs also come with the O spectral type, the sdO stars. They are hotter ($T_{\rm eff}$ between ~40 000 and ~80 000 K) and exhibit a wider range of surface gravities ($\log(g/{\rm cm\,s^{-2}})$ from 4.0 to 6.5). In their majority they have helium-enriched atmospheres[1]. This diversity in properties betrays the very diverse origins of sdO stars. He-poor, compact sdO stars are direct progenies of sdB stars in their immediate post-EHB phase. However, the majority of compact sdO stars are He-rich and are identified as direct post-RGB objects, *i.e* created through the so-called late hot He-flash (Miller Bertolami et al. 2008), or end products of merger events (Webbink 1984; Iben & Tutukov 1984; Iben 1990; Saio & Jeffery 2000, 2002). There are also less compact ($\log(g/{\rm cm\,s^{-2}}) \lesssim 5.0$) sdO stars, which are post-AGB stars, i.e. stars that have ascended

[1] Hot subdwarfs with $T_{\rm eff}$ around 40,000 K mark this transition, and are referred to as sdOB stars. They are often intermediate helium-enriched (iHe-rich) stars.

the asymptotic giant branch after core-He burning exhaustion (Reindl et al. 2016).

Stellar oscillations predicted and discovered in sdB stars by Charpinet et al. (1997) and Kilkenny et al. (1997a), respectively, are among others potentially useful for sdB mass estimations. Pulsating sdB (sdBV) stars reported by Kilkenny et al. (1997a) and in subsequent papers in their series are pressure (p) mode pulsators. Later on, gravity mode (g) and both p and g-mode (called hybrid) sdBVs have been reported by Green et al. (2003) and Baran et al. (2005); Schuh et al. (2006), respectively. Fontaine et al. (2012) compared p- and g-mode sdBVs, clearly indicating that the typical periods of p-mode sdBVs are shorter while amplitudes of a flux variation are higher than of g-mode sdBVs. These two features made a ground-based detection of p-mode sdBVs easier, which led us into a conclusion that p-mode sdBVs are more frequent. Space observations, using *CoRoT*, *Kepler* and *TESS* space observatories revised this statement. Majority of sdBVs detected from space are either g-mode or hybrid with a dominant g-mode component.

Pulsating sdO (sdOV) stars also exist. The very first one, J1600+0748, was identified by Woudt et al. (2006) and exhibits very rapid oscillations from about 60 s to about 120 s. J1600+0748 remained for years the only member of its class despite extensive search among field sdO stars (Rodríguez-López et al. 2007; Johnson et al. 2014). Four sdO pulsators were identified by Randall et al. (2011a) in the globular cluster ω Cen, and over years a couple of more field sdO pulsators were identified, including PB 8783, formerly identified as a common-or-garden sdBV star (Østensen 2012a; Kilkenny et al. 2017a). The periods of all known sdO pulsators are of a few minutes and are consistent with p-mode pulsations (Fontaine et al. 2008).

The goal of this paper is to report our result of the p-mode dominated hot subdwarf stars surveyed by the *TESS* satellite. Since only the Southern Ecliptic hemisphere is already completed using the USC data, our report is limited to that hemisphere only. The Northern Ecliptic hemisphere survey will be reported in the following paper.

2. *TESS* photometry

TESS is deployed in an elliptical, 2:1 lunar synchronous orbit with a period of 13.7 d. Each annual cycle of *TESS* observations are split up into sectors lasting two orbits, or about 27 d. The detector consists of four contiguous CCD cameras, each covering a 24° x 24° field of view (FoV), making up a 24° x 96° strip aligned along ecliptic latitude lines. During Year 1 and 2 the data were stored with the short cadence (SC), lasting 120 s and the long cadence (LC), lasting 1800 s. Since Year 3 there has been additional ultra short cadence (USC) available, lasting 20 s, while the LC was trimmed down to 600 sec. The number of targets observed in the USC and SC is limited and varies from sector to sector. When one sector observations have been completed, the instrument's FoV is shifted eastward by 27°, naturally pivoting around the ecliptic pole. It takes 13 sectors to pivot around one pole, then the FoV is shifted to the other hemisphere for the next cycle. As a result, the regions near the ecliptic poles are observed during every sector and are known as the continuous viewing zones of *TESS*. We downloaded all available data of our targets from the "Barbara A. Mikulski Archive for Space Telescopes" (MAST)[2]. To probe the p-mode region in an amplitude spectrum we are limited to either the SC or USC data. The Nyquist frequency of the former is 4 166 µHz, while of the latter is 25 000 µHz. Our preference is to use the USC data, if available, with which the entire p-mode region is sampled. In the case of the SC data the Nyquist frequency is in the middle of the p-mode region and the aliasing becomes a serious issue. This issue can be sorted out by the finite speed of light, which clearly separates the sub- and super-Nyquist regions in the amplitude spectrum, first discovered by Baran et al. (2012). The amplitudes and profiles of the peaks become different in these both regions, however this effect works only if the data are taken during at least most of the Earth's orbit, and the Nyquist frequency varies significantly enough to modify the signal's reflection across the Nyquist frequency.

We used PDCSAP_FLUX, which is corrected for on-board systematics and neighbors' contributions to the overall flux. We clipped fluxes at 4.5σ to remove outliers, de-trended long term variations (of the order of days) with spline fitting , and calculated an amplitude of a flux variation using the following relation A[ppt]=1000*(flux/<flux>-1).

[2] archive.stsci.edu

3. Fourier analysis

About 4000 hot subdwarfs (and hot subdwarf candidates) have been observed by TESS in both SC and USC monitoring. The list was assembled by members of the Working Group 8 (WG8) of the TESS Asteroseismic Science Consortium (TASC).

Following a recent report by Baran & Koen (2021) we applied a 4.5 times a median noise level detection threshold to both the SC and USC data sets regardless of the data coverage. In the case of one sector data such a threshold corresponds to a confidence level of 5% and 14% for the SC and USC data, respectively. In the case of 0.1% level, the threshold would be around 5.5, hence frequencies below this threshold should be considered tentative. Precise confidence levels for other numbers of sectors can be derived from Equation 5 in Baran & Koen (2021).

We independently searched for p-mode pulsations in these ~ 4000 targets with the FELIX tool (Charpinet et al. 2010; Zong et al. 2016). Firstly, an automatic search was done looking for variations above 1500 μHz in one sector at a time (i.e., without combining sectors for stars having been observed for more than 1 sector), down to a fixed signal-to-noise ratio of 4.8. Secondly, an individual check was carried out on the ~100 candidates to see if detected variations are consistent with p-modes pulsations. In most cases it was not, with a frequent false positive consisting in harmonics of the orbital frequency leaking towards the typical p-mode frequencies. In other cases a single peak, barely emerging (or just at) the defined level of S/N=4.5 was present, and was absent in other sectors in case of re-observations later during the mission, or when combining consecutive sectors on a same star.

We finally detected signals in the p-mode region in 41 objects, agreeing between the two methods for searching for pulsations explained above. Eleven targets were observed only in the SC data, while 30 were observed in the both the SC and USC data, though only the USC data were utilized. We found 10 new detections in the SC data and 10 new detections in the USC data, while the remaining 1 (SC) and 20 (USC) sdVs were known prior to the *TESS* observations. We present the full list of p-mode sdVs in Table 1. Below, we describe each target providing prior knowledge on the pulsation properties and including amplitude spectra and list of frequencies we have detected.

3.1. Targets observed in the SC mode

TIC 10011123 (TYC 4824-1038-1 = Gaia DR3 3058814547877917056) is a new pulsating sdOB

Table 1: Observational log. Sectors we used in our analysis are marked with **bold**.

TIC	SC Sector	USC Sector	sd type	detection
10011123	**33**	–	sdOB	new
19690565	**34**	–	sdBO	new
139481265	**33**	–	sdB	new
142200764	**3**	–	sdB	known
143699381	**13**	–	sdB	new
289149727	**38**	–	sdBO	new
295046932	**39**	–	sdBO	new
366656123	**34**,**44**	–	sdB	new
387107334	**13**	–	sdB	new
408147637	**38**	–	sdBO	new
455095580	**34**	–	sdB	new
29840077	1,28	**28**	sdB	new
33318760	8,35	**35**	sdB	known
47377536	9,35,46	**35**,**46**	sdB	known
53826859	33	**33**	sdB	new
60257911	44,45,46	**44**,**45**,**46**	sdB	known
62381958	1,30	**30**	sdOB	known
62483415	1,28	**28**	sdOB	known
69298924	44,45,46	**44**,**45**,**46**	sdB	known
70549283	44,45,46	**44**,**45**,**46**	sdOB	new
98871628	10,36	**36**	sdB	known
139723188	1,27,28	**27**,**28**	sdOB	known
156618553	46	**46**	sdB	known
169285097	2,29	**29**	sdB	new
220573709	1,2,3,28,30	**28**,**30**	sdO	known
241771689	38	**38**	sdB	new
248949857	3,30	**30**	sdO	known
273218137	10,37	**37**	sdB	new
322009509	2,29	**29**	sdOB	known
335635628	46	**46**	sdB	known
355058528	27	**27**	sdB	known
355638102	1,2,28	**28**	sdO	new
366399746	45,46	**45**,**46**	sdB	new
396954061	5,32	**32**	sdB	known
409644971	13,39	**39**	sdB	new
434923593	38	**38**	sdB	known
436579904	5,32,43,44	**32**,**43**,**44**	sdB	known
437043466	44,45,46	**44**,**45**,**46**	sdB	known
452718256	9,36	**36**	sdOB	known
471013461	4,31	**31**	sdB	new
673345538	43,44	**43**,**44**	sdB	known

star (sdOBV). The sdB classification is confirmed with a spectrum taken with the 1.9 m telescope at the South African Astronomical Observatory (SAAO). Details of all classifications obtained by means of SAAO spectra can be found in the paper by Kilkenny et.al., which is currently under preparation. *TESS* observed the star during Sector 33. An amplitude spectrum shown in Fig. 1 delivers three peaks in the g-mode region and one peak in the high frequency region. Since the target was observed during just one sector we are unable to separate a real frequency from its alias across the Nyquist frequency. We show the list of the prewhitened frequencies in Table 2. Since the majority of p-modes detected in sdBVs are above 4000 µHz we have arbitrarily prewhitened frequencies in the super-Nyquist region. Based on previous detections of p-mode sdBVs we can see a correlation between the effective temperature and the frequencies of p-modes. The lower the temperature is the lower the frequencies at which signals can appear. Unfortunately, the frequency jitter is still up to a few thousand of µHz, hence we cannot apply this rule based only on $T_{\rm eff}$. To verify our frequency choice for targets observed in the SC only, we need either the USC data or additional at least one sector SC data. The latter argument is clearly seen for TIC 366656123.

TIC 19690565 (Gaia DR3 5753155495252812544) is a new sdBOV star. We use BO designation in the case either sdB or sdOB is possible. This is caused by low S/N of a spectrum, not allowing for concluding on a detection of helium lines. Our fit to a spectrum taken with the 2.54 m Nordic Optical Telescope (NOT) in 2015 gives $T_{\rm eff}$ = 31 150(300) K, log (g/cm s^{-2}) = 5.765(47), and log(n(He)/log (H)) < -3.23(16). *TESS* observed the star during Sector 34. We detected two peaks closed to the Nyquist frequency and we selected the one in the super Nyquist region. We show the amplitude spectrum in Fig. 1, and we list the prewhitened frequencies in Table 2.

TIC 139481265 (Gaia DR3 3342874205845523072) is a new sdBV star. Our fit to a spectrum taken with the NOT in 2018 gives $T_{\rm eff}$ = 31 810(540) K, log (g/cm s^{-2}) = 5.80(4), and log(n(He)/log n(H)) = -2.24(8), indicating a sdB classification. *TESS* observed the star during Sector 33. We found three peaks and we have chosen those located in the super Nyquist region. The frequencies are listed in Table 2. They are close to each other and the separation between the adjacent ones are 1.55(3) and 1.60(5) µHz, respectively between the two lowest and the two highest frequencies. The frequency spacing is equal within the errors, which can indicate that these three peaks can constitute a rotationally split triplet. If our interpretation is correct the rotation period would be equal to 7.35(27) days. We show an amplitude spectrum in Fig. 1.

TIC 142200764 (HE 0230–4323 = Gaia DR3 4947023428379-802752) was found by Edelmann et al. (2005) to be a binary system with an sdB as the primary component. The authors reported a binary period of 0.4515(2) days, a systemic velocity of 42.3(3) km/s, and a radial velocity amplitude of 109.6(4) km/s. They concluded that the companion to the sdB star is either a main sequence or a white dwarf companion, depending on the orbit's inclination and the mass of the sdB. Koen (2007) confirmed the binarity photometrically and detected pulsations in the sdB star, calling it an unusual pulsating star because the pulsation frequencies changed over the course of several nights from ~32–39 d^{-1} to ~8–16 d^{-1}. Kilkenny et al. (2010) revisited the system, confirming the binarity and explaining the unusual g-mode pulsations as an under-sampling error. In fact, the authors reported on a discovery of short period pulsations. *TESS* observed the star during Sector 3. We recovered the orbital frequency and its first harmonic associated with binarity. The phase-folded light curve is shown in Fig. 2, and the ephemeris is provided in Table 3. The light curve is dominated by a reflection effect, which points at the main sequence star to be a companion. In addition, we found eight frequencies in the p-mode region. We show an amplitude spectrum with two close-ups in Fig. 1. Since the star was observed in the SC, we would not be able to discern between the real frequencies and their aliases across the Nyquist frequency, if the frequencies were not reported by Kilkenny et al. (2010). In this case these are the frequencies in the sub-Nyquist region that are real. Two frequencies, f_4 and f_8 should be considered tentative since their amplitudes are below our adopted detection threshold, and were also not detected by Kilkenny et al. (2010). Frequency

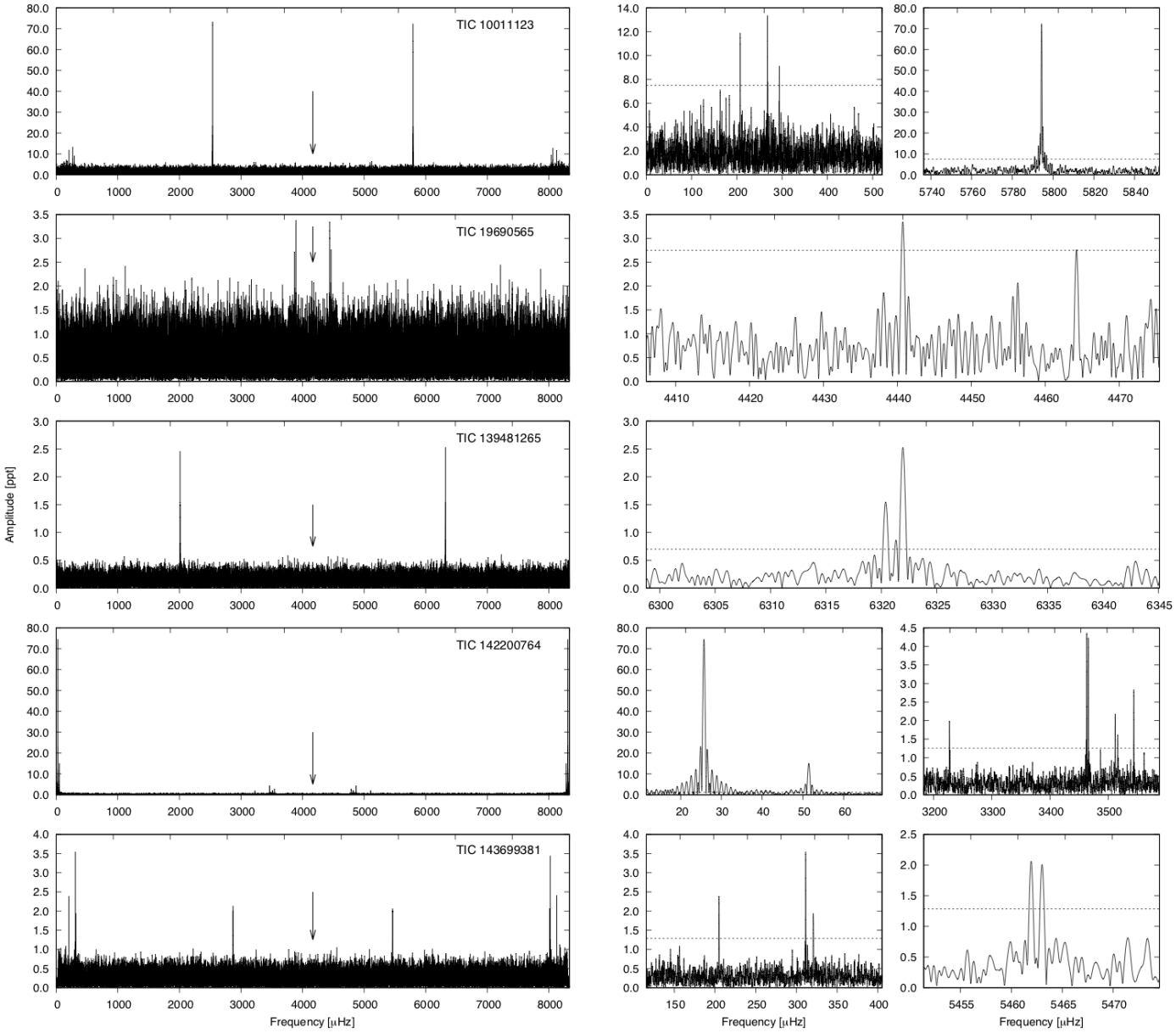

Fig. 1: *Left panels:* Amplitude spectra, up to twice the Nyquist frequency, of the targets observed in the SC. The arrows point at the Nyquist frequency of 4166.67 μHz. *Right panels:* close-ups at the detected frequencies.

f_5 was also not detected by the authors. On the other hand, we have not detected frequencies above 5700 μHz, which were detected by the authors. The full list of frequencies we detected in *TESS* data is shown in Table 2.

TIC 143699381 (Gaia DR3 6715490300005795840) is a new sdBV star. This classification is obtained with a spectrum taken with the 1.9 m telescope at SAAO. *TESS* observed the star during Sector 13. We detected five frequencies, three in the g-mode region and two in the p-mode region, which make the star a hybrid sdBV. We show an amplitude spectrum in Fig. 1, and we list the prewhitened frequencies in Table 2.

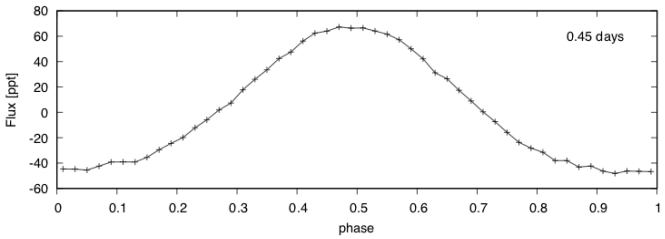

Fig. 2: Phase-folded light curve of TIC 142200764 showing a reflection effect. The number in the upper right corner is the orbital period, rounded to two significant digits, used for folding the light curve.

TIC 289149727 (Gaia DR3 5870233314477487872) is a new sdBOV star. This classification is obtained with a spectrum taken with the 1.9 m telescope at SAAO. *TESS* observed the star during Sector 38. We detected four frequencies, one low frequency and three frequencies in the p-mode region. The low frequency is not typical of pulsations in sdBV stars and it is likely a signature of a

Table 2: List of frequencies we detected in the targets observed only with the SC.

ID	Frequency [μHz]	Period [sec]	Amplitude [ppt]	S/N
		TIC 1001123		
f_1	207.365(29)	4822.4(7)	11.9(1.4)	7.1
f_2	267.617(25)	3736.68(36)	13.3(1.4)	8.0
f_3	293.892(37)	3402.62(43)	9.1(1.4)	5.4
f_4	5794.3287(47)	172.58255(14)	72.4(1.4)	43.2
		TIC 19690565		
f_1	4440.736(38)	225.1879(19)	3.3(5)	5.5
f_2	4464.242(47)	224.0022(23)	2.8(5)	4.5
		TIC 139481265		
f_1	6320.398(29)	158.2179(7)	1.12(13)	7.3
f_2	6321.948(14)	158.17908(35)	2.45(14)	15.8
f_3	6323.546(45)	158.1391(11)	0.72(13)	4.7
		TIC 142200764		
f_{orb}	25.7194(9)	38881.2(1.4)	74.81(24)	266.2
$2f_{orb}$	51.438743	19440.599451	15.06(24)	53.6
f_1	3227.112(36)	309.8746(34)	2.06(24)	7.3
f_2	3463.071(18)	288.7611(15)	4.15(24)	14.8
f_3	3465.906(18)	288.5248(15)	4.02(24)	14.3
f_4	3486.66(7)	286.807(5)	1.12(24)	4.0
f_5	3511.989(33)	284.7389(27)	2.21(24)	7.9
f_6	3516.297(40)	284.3901(33)	1.82(24)	6.5
f_7	3543.983(27)	282.1684(22)	2.72(24)	9.7
f_8	3561.62(6)	280.771(5)	1.15(24)	4.1
		TIC 143699381		
f_1	204.923(24)	4879.9(6)	2.38(24)	8.3
f_2	311.308(16)	3212.25(17)	3.53(24)	12.4
f_3	320.615(30)	3119.01(29)	1.94(24)	6.8
f_4	5461.957(33)	183.0846(11)	1.90(24)	6.7
f_5	5462.990(34)	183.0500(11)	1.85(24)	6.5
		TIC 289149727		
f_1	50.769(20)	19696.9(7.6)	29.9(2.5)	10.3
f_2	5527.456(12)	180.91506(39)	49.9(2.5)	17.2
f_3	5529.050(9)	180.86288(30)	65.5(2.5)	22.5
f_4	5546.945(19)	180.2794(6)	31.2(2.5)	10.7
		TIC 295046932		
f_1	5524.300(38)	181.0184(12)	8.7(1)	5.1
f_2	5551.400(14)	180.13473(46)	23.4(1)	13.7
f_3	6059.790(19)	165.0222(5)	17.5(1)	10.2
f_4	6177.657(12)	161.87367(31)	27.9(1)	16.3
f_5	6229.586(32)	160.5243(8)	10.4(1)	6.0
f_6	6208.480(10)	161.07001(26)	34.4(1)	20.1
f_7	6207.534(12)	161.09456(30)	29.0(1)	16.9
f_8	6210.064(33)	161.0289(8)	10.3(1)	6.0
f_9	6260.176(14)	159.73992(36)	23.5(1)	13.7
f_{10}	6358.416(39)	157.2719(10)	8.5(1)	5.0
f_{11}	6452.331(26)	154.9828(6)	12.5(1)	7.3
		TIC 366656123 - Sector 34		
f_1	34.384(6)	29083.2(4.7)	15.47(35)	38.0
f_2	3430.220(33)	291.5265(28)	2.62(35)	6.4
		TIC 387107334		
f_1	5230.956(23)	191.1696(8)	3.64(38)	8.1
		TIC 408147637		
f_1	24.963(23)	40059(37)	5.2(5)	8.6
f_2	323.644(41)	3089.81(39)	3.0(5)	4.9
f_3	5340.857(28)	187.2359(10)	4.3(5)	7.1
f_4	5389.176(33)	185.5571(11)	3.7(5)	6.0
f_5	5537.739(29)	180.5791(10)	4.2(5)	6.8
		TIC 455095580		
f_1	4461.092(36)	224.1604(18)	4.1(6)	5.8

Table 3: Ephemerides for three stars showing a reflection effect.

TIC	Reference epoch [BJD]	Period [days]
142200764	2458386.7338(10)	0.450060(39)
409644971	2458657.06556(34)	0.090740491(12)
436579904	2458438.90745(38)	0.39800589(18)

binarity rather than a g-mode. We show an amplitude spectrum in Fig. 3, and we list the prewhitened frequencies in Table 2.

TIC 295046932 (Gaia DR3 5811947687666193280) is a new sdBOV star. Likewise in the previous two targets, this classification is obtained with a spectrum taken with the 1.9 m telescope at SAAO. *TESS* observed the star during Sector 39. We detected 11 frequencies in the p-mode region. We show an amplitude spectrum in Fig. 3, and we list the prewhitened frequencies in Table 2.

TIC 366656123 (Gaia DR3 5951282650153931 52 = SDSS J084122.66+063029.6) is a new sdBV star. Our fit to a spectrum taken with the 2.5 m Sloan Digital Sky Survey (SDSS) telescope in 2008 gives $T_{\rm eff}$ = 31 300(200) K, $\log(g/{\rm cm\,s^{-2}})$ = 5.56(3), and log(n(He)/ n(H)) = -2.8(1). It was included in a sample of hot subdwarf candidates analyzed by Sahoo et al. (2020a). The authors detected a low frequency and consequently the object has been proposed and successfully observed by *TESS* during Sectors 34 and 44. The data are too far apart to combine them together and analyze as one piece since the Fourier window function will be very complex. Instead, we analyzed these two data sets separately and compared the signal detected. In both sectors we have detected one frequency in the g-mode region and one high frequency in the p-mode. We show an amplitude spectrum calculated only from Sector 34 data in Fig. 3. To be consistent with analysis of other targets we should pick the frequency in the super Nyquist region, however the high frequency is shifted between sectors. We show it in Fig. 4. The middle panel shows that the Nyquist frequency is shifted between sectors, which will consequently shift the reflections of frequencies. Indeed, the frequencies in the super-Nyquist region are not aligned, which we interpret as reflections, and therefore the signal at high frequency originates in the sub-Nyquist region. This also confirms that our arbitrary choice of selecting peaks in the super-Nyquist region may not always be correct. We list the prewhitened frequencies in Table 2.

TIC 387107334 (Gaia DR3 6439287618985307776 = BPS CS 22959-140) is a new sdBV star. It was originally classified as an sdO subdwarf in the BPS catalog (Beers et al. 1992), however a spectrum taken with the 1.9 m telescope at SAAO points at a sdB classification. *TESS* observed the star during Sector 13. We detected only a single frequency in the p-mode region. We show an amplitude spectrum in Fig. 3, and we list the prewhitened frequency in Table 2.

TIC 408147637 (Gaia DR3 5867781918951429760) is a new sdBOV star. This classification is obtained with a spectrum taken with the 1.9 m telescope at SAAO. *TESS* observed the star during Sector 38. We detected five frequencies, one low frequency, one in the g-mode region and three in the p-mode region. We show an amplitude spectrum in Fig. 3, and we list the prewhitened frequencies in Table 2.

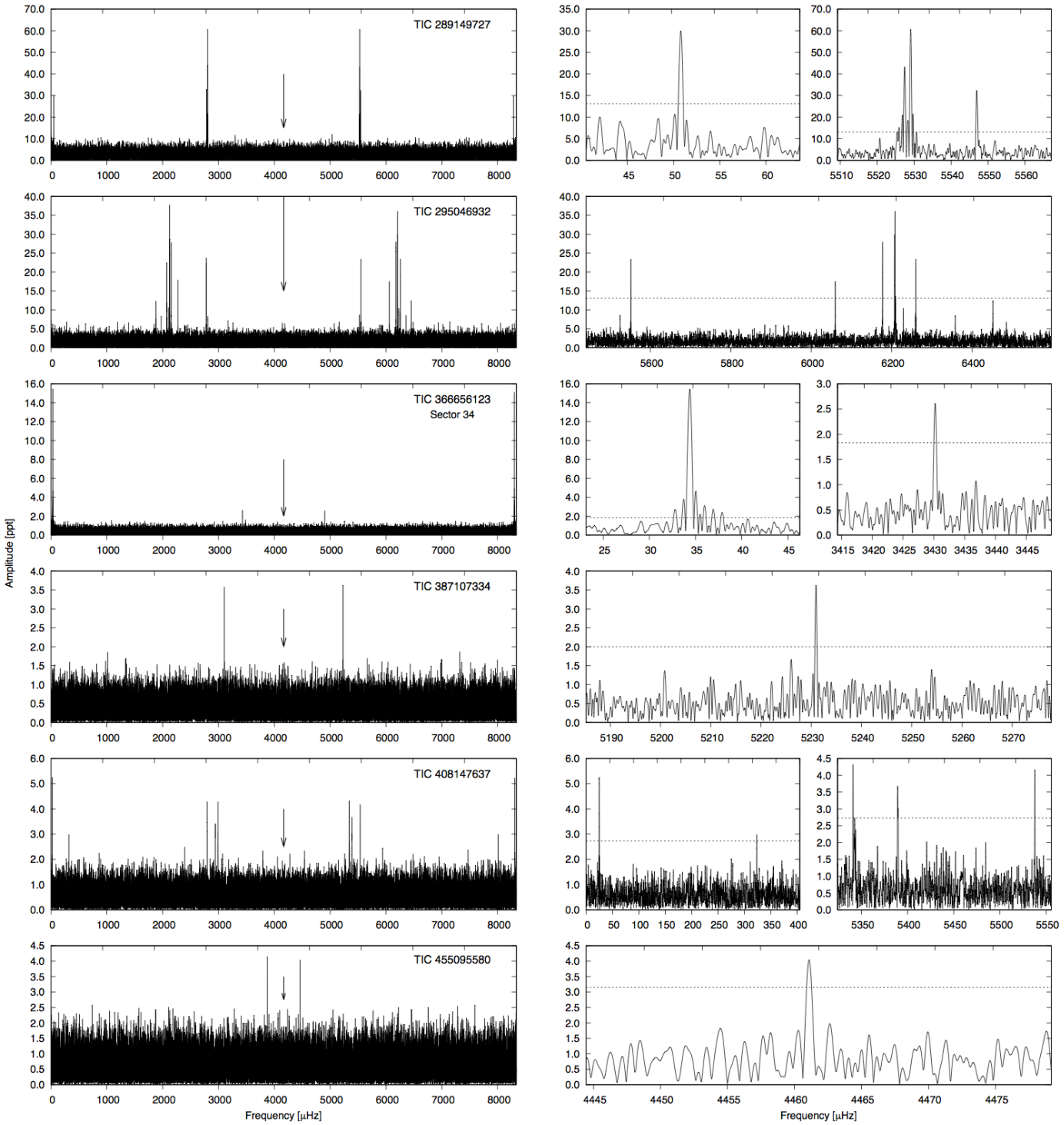

Fig. 3: Same as in Fig. 1 but for another five targets observed only in the SC.

TIC 455095580 (Gaia DR3 3096564462848659328) is a new sdBV star. Our fit to a spectrum taken with the NOT in 2022 gives $T_{\rm eff} = 30\,800(500)$ K, $\log(g/{\rm cm\,s^{-2}}) = 5.7(1)$, and log(n(He)/log (H)) = -2.55(15), indicating an sdB classification. *TESS* observed the star in Sector 34. We detected only one frequency in the p-mode region. We show an amplitude spectrum in Fig. 3, and we list the prewhitened frequency in Table 2.

3.2. Targets observed in the USC mode

For all targets observed in USC mode there is also corresponding SC data available. In addition, some targets listed below were observed during specific sectors (1-13) in SC only. Since the USC data are providing us with a unique frequency identification, we have decided not to analyze any SC data including those taken in sectors without simultaneous USC monitoring. Table 1 provides detailed sector information and we will not mention sectors with the SC data below.

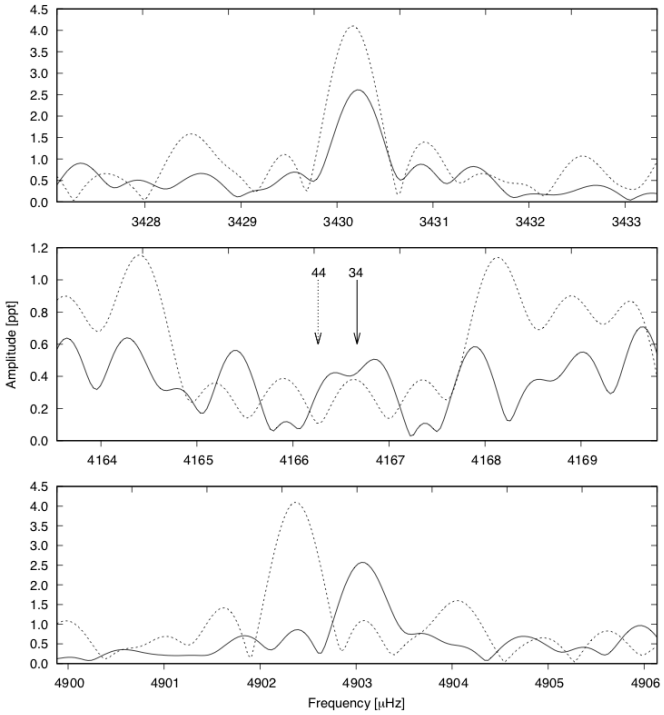

Fig. 4: *Top panel:* a close up of the amplitude spectrum of TIC 366656123 showing a high frequency in the sub-Nyquist region; solid and dashed lines represent Sector 34 and 44, respectively. *Middle panel:* shows the Nyquist frequency region. The arrows point at the Nyquist frequency in Sectors 34 and 44. *Bottom panel:* a close up of the amplitude spectrum showing a high frequency in the super-Nyquist region.

TIC 29840077 (Gaia DR3 6803823552347267968, EC 21032-2551) is a new sdBV star. This target was identified as sdB star by O'Donoghue et al. (2013). *TESS* observed the star during Sector 28. We detected two frequencies in the p-mode region. We show an amplitude spectrum in Fig. 5, and we list the prewhitened frequencies in Table 4.

TIC 33318760 (Gaia DR3 3766481985523752320, V541 Hya, EC 09582–1137, PG 0958–116) is a known sdBV star. It was included in the catalog of UV-excess stellar objects (Green et al. 1986) and in the catalog of spectroscopically identified hot subdwarfs (Kilkenny et al. 1988, 1997b). Kilkenny et al. (2006) analyzed the photometric data and reported a detection of two frequencies in the p-mode region. Additional four significant frequencies were reported by Randall et al. (2009). One of the modes was considered split by rotation. The authors preformed period fit and obtained structural parameters of the sdB. Mackebrandt et al. (2020) searched, with a null result, for a change in arrival time of stellar pulsations induced by a sub-stellar companion. *TESS* observed the star during Sector 35. We detected one frequency (f_1) in the intermediate frequency region and two frequencies (f_2, f_3) in the p-mode region. Frequency f_1 is of low amplitude and could be noise-induced. Likewise f_2. These two frequencies had not been detected from the ground. Frequency f_3 confirms the highest frequency reported by both Kilkenny et al. (2006) and Randall et al. (2009). Its amplitude is much smaller in the *TESS* data as compared to the ground observations. We show an amplitude spectrum in Fig. 5, and we list the prewhitened frequencies in Table 4.

TIC 47377536 (Gaia DR3 3806303066866089216, UY Sex, PG 1047+003) is a known sdBV star and has been extensively studied since its independent discovery by Billères et al. (1997) and O'Donoghue et al. (1998). Five and eight independent frequencies were reported by the former and latter authors, respectively. O'Donoghue et al. (1998) confirmed all frequencies reported by Billères et al. (1997). Kilkenny et al. (2002) reported enhanced list of frequencies obtained from the multisite campaign. The authors listed 18 frequencies, however three reported by O'Donoghue et al. (1998) were not detected. Kilkenny et al. (2002) speculated on rotationally split modes and provided a mode identification and a comparison of modeled and observed periods. Charpinet et al. (2003) published a model providing mode identifications for 16 frequencies. The star was observed during the *Kepler K2* mission (Reed et al. 2020). The authors detected 97 frequencies, including rotationally split multiplets. The frequency splitting allowed for a rotation period of 24.6(3.5) days to be estimated. The authors reported all frequencies detected prior to their analysis. *TESS* observed the star in Sectors 35 and 46. We analyzed both sectors separately. Since we have not detected all frequencies in both sectors, while the amplitudes of those repeating in both sectors are different, we have decided not to merge data for a joint analysis. Merging would average amplitudes and contribute with a complex window function, making prewhitening difficult. In both sectors we detected only 13 independent frequencies. Majority of frequencies confirm the ones reported by Reed et al. (2020), however even accounting for a poor frequency resolution, which is around 0.5 μHz, we report f_7 in Sector 35 and f_4,f_5 in Sector 46 as new detections. We show an amplitude spectra calculated only from Sector 46 data in Fig. 5, and we list the prewhitened frequencies in Table 4.

TIC 53826859 (Gaia DR3 2921084812241684608) is a new sdBV star. The sdB classification is confirmed with a spectrum taken with the 1.9 m telescope at SAAO. *TESS* observed the star during Sector 33. We detected 11 frequencies in the p-mode region. The frequencies are rather low for p-modes. We show an amplitude spectrum in Fig. 5, and we list the prewhitened frequencies in Table 4.

TIC 60257911 (Gaia DR3 6563455333986384640) is a known sdBV star. Reed et al. (2018) found the star to be a binary consisting of an sdB and a main-sequence companion. The authors analyzed *K2* data and reported 16 frequencies in the p-mode region. Just a few candidates for rotationally split modes were marked and a possible 11.5(8) days spin rate was estimated. *TESS* observed the star during Sectors 44, 45 and 46. We detected only two frequencies, which were found in the *K2* data to be the highest amplitude frequencies. We do not confirm our frequency f_2 to be rotationally split. The *TESS* data coverage of ~79 days is comparable to the coverage obtained with the *K2*. We show an amplitude spectrum in Fig. 5, and we list the prewhitened frequencies in Table 4.

TIC 62381958 (Gaia DR3 5149241067178231552, EC 01541-1409) is a known sdOBV star. It was mentioned to be a sdOB star by Kilkenny et al. (2009), and included in the spectroscopically identified hot subdwarfs catalog later by Kilkenny et al. (2016). Kilkenny et al. (2009) analyzed photometric data and reported a list of six frequencies in the p-mode region. A follow-up multiste time series data were collected and analyzed by Reed et al. (2012). The number of frequencies reported depends on an ob-

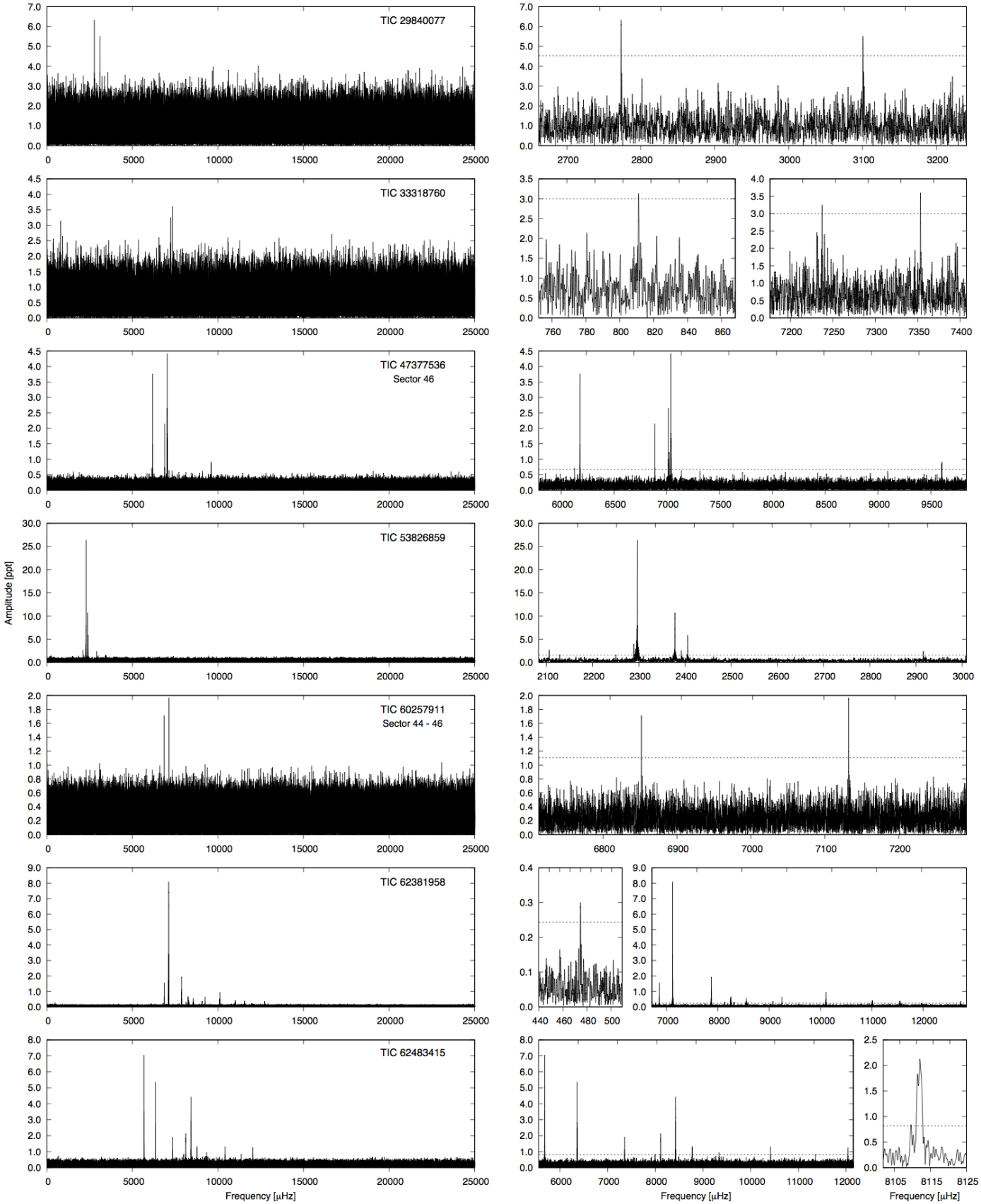

Fig. 5: *Left panels:* Amplitude spectra, up to the Nyquist frequency, of targets observed in the USC. *Right panels:* close ups at the detected frequencies.

servational season but reaches almost 30 in 2009. All frequencies reported by Kilkenny et al. (2009) were detected by Reed et al. (2012). The time span of the 2009 multisite campaign is around a month, still the authors reported no candidates rotationally split frequencies. Randall et al. (2014) reported results of a mode identification of several frequencies detected in the spectrophotometric data collected by the authors. *TESS* observed the star during Sector 30. We show an amplitude spectrum in Fig. 5, and we list the prewhitened frequencies in Table 4. The majority of frequencies we detected overlap with those listed by Reed et al. (2012). In addition we found one significant frequency in the g-mode region at a relatively high frequency. Such a frequency in this star has not been reported thus far. As it was shown by Reed et al. (2012) this exhibits frequency/amplitude variation of the pulsations modes between two observational seasons. The signal in the amplitude spectrum calculated from the *TESS* data is also very unstable. We tried to prewhiten all signal down to the adopted threshold, however we are not convinced the close frequencies, within 1 µHz, are independent or a consequence of an instability of one mode. A common frequency spacing between close frequencies is about 0.5 µHz, which is comparable to the frequency resolution of derived from 1/T, with T being a total data coverage. Since the data are quite continuous the aliases in a Fourier window response are of low amplitudes, hence we do not expect the close frequencies are aliases.

TIC 62483415 (Gaia DR3 6601695863046409600, PHL 252, EC 22221-3152) is a known sdOBV star. Kilkenny (1987); Kilkenny et al. (2016) listed the star in the catalog of spectroscopically identified hot subdwarfs. Kilkenny et al. (2009) observed it photometrically and reported 11 frequencies between 5 500 and 11 900 µHz. It was not mentioned in the paper but f_{11} looks like the first harmonic of f_1. Barlow et al. (2017) delivered two-site photometry of the star and reported 11 independent frequencies along with three combination and four close frequencies, which the authors interpreted as rotationally split modes. The rotation period was estimated at ~8 days but this is an incorrect statement (see below). *TESS* observed the star during Sector 28. We detected 10 independent as well as two combination frequencies. We show an amplitude spectrum in Fig. 5, and we list the prewhitened frequencies in Table 4. We found f_{11} and f_{12} not detected by the other authors. The rotation period derived by the latter authors is close to their data coverage and that is why they suggested longer timebase to confirm this result. One sector *TESS* data is roughly 27 days. If the rotation period is indeed about 8 days we should surely detect split modes. They listed their f_1 and f_5 as candidates for split modes. We find the former frequency (f_5 in our list) to be an amplitude variable, and the latter frequency (f_6 in our list) to be single. Frequency f_5 in our list is so variable that we were unable to prewhite any frequency in that range and decided to quote numbers red by eye, hence without error estimates.

TIC 69298924 (Gaia DR3 6548668234011111168) is a known sdBV star. Vennes et al. (2011) identified the star as sdB, while Baran et al. (2011a) analyzed photometric data reporting four frequencies, two in the g-mode and two in the p-mode region. That detection made the star a hybrid sdBV. The authors analyzed time-series spectroscopic data detecting one frequency, which overlaps with the highest amplitude frequency in the photometric data. *TESS* observed the star during Sector 44, 45 and 46. Since these are consecutive sectors and the amplitude spectra calculated from single sector data do not differ substantially, we combined all data together. We detected four frequencies in the p-mode region and none in the g-mode region. Three frequencies are close to each other and looks like a rotationally split frequencies. The average frequency splitting of 0.8953(67) µHz translates into the rotation period of 12.9(1) days. These three frequencies overlap with, apparently unresolved, frequency f1 reported by Baran et al. (2011a). Our frequency f_1 is close to frequency f_1 reported earlier. We show an amplitude spectrum in Fig. 6, and we list the prewhitened frequency in Table 4.

TIC 70549283 (Gaia DR3 6730585568167962 88) is a new sdOBV star. The spectral classification was reported by Lei et al. (2019). *TESS* observed the star during Sectors 44 – 46. We detected only one frequency. We show an amplitude spectrum in Fig. 6, and we list the prewhitened frequency in Table 4.

TIC 98871628 (Gaia DR3 3486707300467202304, V551 Hya, EC 11583-2708) is a known sdBV star. Kilkenny et al. (1997b) listed the star in the catalog of spectroscopically confirmed hot subdwarfs and reported a composite spectrum. The pulsations were found by Kilkenny et al. (2006). The authors detected four frequencies. *TESS* observed the star during Sector 36. We detected only one frequency, which is the one with the highest amplitude reported by Kilkenny et al. (2006). We show an amplitude spectrum in Fig. 6, and we list the prewhitened frequency in Table 4.

TIC 139723188 (Gaia DR3 6466786576593357440, EC 21281-5010) is a known sdOBV star. Kilkenny et al. (2015) identified the star to be a hot subdwarf. Kilkenny et al. (2019) observed it photometrically and reported three frequencies. *TESS* observed the star during Sector 27 and 28. Since these are consecutive sectors and the amplitude spectra calculated from single sectors show very similar signal distribution, we analyzed these two sectors merged together. We detected three frequencies, but only two are the same as reported by Kilkenny et al. (2019). We show an amplitude spectrum in Fig. 6, and we list the prewhitened frequencies in Table 4.

TIC 156618553 (Gaia DR3 3675067076961979264, HW Vir, PG 1241-084, HE 1241-0823) is a known sdBV star. It has been extensively studied in the past. Berger & Fringant (1980) classified the object as sdB, while Kilkenny et al. (1988) confirmed this type and found it to be a binary system. Since that time the object has been monitored mostly photometrically to verify the stability of the orbital period. We estimated the mid-times of eclipses observed by *TESS* and derived the orbital period of 0.116719509(8) days. Baran et al. (2018) found the sdB star to be a rich pulsator, reporting both the g- and p-mode pulsations. In total, they listed 91 frequencies, majority in the g-mode region, with a decent number in the intermediate region and only three above 3000 µHz. The authors delivered the most updated Observed–Calculated diagram at the time. *TESS* observed the star during Sector 46. We removed the orbital contribution in the amplitude spectrum prior to pulsation search. Finally, we detected only four frequencies, with one being in the p-mode region. Only one frequency f_2 we detected in the *TESS* data overlaps with f_4 listed by Baran et al. (2018). We show an amplitude spectrum in Fig. 6, and we list the prewhitened frequencies in Table 4. We have also removed the pulsations from the data to derive mid-times of eclipses. We folded all eclipses within a single *TESS*

orbit and derived the following mid-times, 2 459 559.135104(1) and 2 459 572.908007(1), during the first and the second *TESS* orbits, respectively.

TIC 169285097 (Gaia DR3 2312392250224668288, HE 2341-3443, CD-35 15910) is a new sdBV star. It has been listed as a sdB star by Lamontagne et al. (2000). During the *TESS* mission, it has been first observed by *TESS* during Sector 2 and the results of pulsation analysis was reported by Sahoo et al. (2020b). The authors analyzed only the SC data reporting 43 frequencies, with six being high frequencies. The *TESS* photometry was also taken during Sector 29 in both the SC and USC. We analyzed both cadences and detected the same frequencies. We provide the results obtained in the USC. We list the frequencies in Table 4 and we show an amplitude spectrum in Fig. 6. We detected only 34 frequencies, which is short by nine compared to the list reported by Sahoo et al. (2020b). We did not find any new frequencies in Sector 29.

TIC 220573709 (Gaia DR3 4720417758386878080, EC 03089-6421) is a known sdOV star. Kilkenny et al. (2015) listed the star in the catalog of spectroscopically hot subdwarfs. Kilkenny et al. (2017b) reported very high frequencies, one ~32.12 mHz and the other ~29.26 mHz, detected in the photometric data. The authors speculated that this star can be a field counterpart of the ω Cen sdO variables (Randall et al. 2011b). Next, Kilkenny et al. (2019) reobserved it and besides those two frequencies, they found additional one of ~37.65 mHz. *TESS* observed the star during Sectors 28 and 30. The USC delivers the Nyquist frequency short of the frequencies reported by Kilkenny et al. (2017b, 2019), so if not these reports, and we detect any frequencies, these would surely be aliases of frequencies reported from the ground. The amplitude spectra look a little differently between sectors hence the window function of combined data gives averaged amplitudes and split peaks, which are not helping during prewhitening. We have decided to analyze each sector data separately. We show an amplitude spectrum calculated only from Sector 28 data in Fig. 6, and we list the prewhitened frequencies in Table 4. In both sectors we confirm frequencies around 32.12 mHz, while we detected 29.26 mHz frequency only in Sector 28. We found no signature of the highest frequency around 37.65 mHz. Besides the high frequencies, in both sectors, we detect ~12.1 μHz frequency. Such a low frequency can be attributed either to a binary frequency or an on-board systematics. We know of ~1c/d artifact, which is related to Earth's rotation. However, the high frequencies are spaced exactly by the low frequency value. To interpret both the low frequency and the spacing between high frequencies we can invoke a tidally lock binary system. In such case, the rotation, determined by the frequency splitting between rotationally split frequencies would be the same as the binary frequency. If this interpretation is correct the star has the shortest rotation period among all subdwarfs for which the rotation has been estimated.

TIC 241771689 (Gaia DR3 6093621087563287040, CD-48 8608) is a new sdBV star. It is included in the GALEX survey (Németh et al. 2012). Kawka et al. (2015) listed the star as a binary system consisting of a sdB and a G8 main sequence companion. *TESS* observed the star during Sector 38. We show an amplitude spectrum in Fig. 7. It is very rich in frequencies in the p-mode region. We also detected six frequencies in the g-mode region, so the star is a hybrid pulsator. The list of prewhitened frequencies is shown in Table 4. The highest amplitude frequencies ~5120 μHz show a multiplet structure and there are two frequency splittings that we can report. The splitting between frequencies f_{10}, f_{12} and f_{15} is ~17 μHz, while the splitting between f_9, f_{10} and f_{11}, f_{12} and f_{13}, f_{15} and f_{16} is ~1.5 μHz. Surprisingly, we detect a few low amplitude frequencies between 10 and 40 μHz, including 15.7 μHz and its first harmonic, and 17.4 μHz and its first harmonic. The frequencies are not included in our list of prewhitened frequencies. If we assume the splitting of ~17 μHz is caused by rotation, the rotation period would be ~0.7 days, which is the shortest among rotation periods estimated in other sdBV stars. If, on the other hand, the splitting of ~1.5 μHz is caused by rotation, then the period would be ~7.7 days, which is comparable to *e.g.* the one estimated for V585 Peg (Baran et al. 2009). Some of the frequencies above 10 000 μHz can be combination frequencies of the highest amplitude modes. We found no exact values, however f_{42} is very close to $2 \cdot f_{15}$ while f_{41} is close to $f_{10}+f_{15}$.

TIC 248949857 (Gaia DR3 2482171590176492928, EO Cet, PB 8783) is a known sdOV star. It has been originally identified as a sdB star in which pulsations were found by Koen et al. (1997). The authors reported six high frequencies. Subsequent paper by O'Donoghue et al. (1998) reported 11 frequencies, including close resolved frequencies, as a consequence of a higher frequency resolution, but did not confirm 7.883 and 8.291 μHz frequencies. The authors provided a mode identification by fitting models to the observed periods. Østensen (2012b) analyzed new spectra and reclassified this star as a sdO star. *TESS* observed the star during Sector 30. We detected 11 frequencies, confirming detections reported by O'Donoghue et al. (1998) and Van Grootel et al. (2014). We show an amplitude spectrum in Fig. 7, and we list the prewhitened frequencies in Table 4.

TIC 273218137 (Gaia DR3 5371215147518355328) is a new sdBV star. It was mistakenly identified as a white dwarf by McCook & Sion (1987). Kawka et al. (2007) collected new spectroscopy and reclassified the object as a sdB star, with $T_{\rm eff} = 30\,080(660)$ K, $\log (g/{\rm cm\,s^{-2}}) = 5.15(10)$, and $\log({\rm n(He)/log\,(H)}) \geq -3.0$. *TESS* observed the star during Sector 37. We detected a large amplitude high frequency with two low amplitude frequencies symmetrically spaced by 3.696(21) μHz, on average. If we interpret these three frequencies (f_4,f_5,f_6) as rotationally split modes, then the rotation period we derive equals 3.132(18) days. Besides high frequencies, which we can interpret as p-modes, we detected three frequencies in the g-mode region (f_1,f_2,f_3). Two types of modes make this star to be a hybrid sdBV, which should have been expected based on $T_{\rm eff}$ and log g estimates. We also detected a very low frequency, which cannot be interpreted as pulsations. We tentatively mark this frequency as binary related, however this interpretation should be confirmed with future data. The orbital period would be equal to 5.713(11) days. We show an amplitude spectrum in Fig. 7, and we list the prewhitened frequencies in Table 4.

TIC 322009509 (Gaia DR3 4990641054653089664, JL 166) is a known sdOBV star. Kilkenny et al. (1988) listed the star as sdOB. Barlow et al. (2009) reported 10 frequencies and one combination frequency. *TESS* observed the star in Sector 29. We show an amplitude spectrum in Fig. 7, and we list the prewhitened frequencies in Table 4. We detected only two frequencies and none of them were previously reported by the latter authors, although they are close to their f_2 and f_4.

TIC 335635628 (Gaia DR3 3609593392911348096, PG 1315-123) is a known sdBV star. Green et al. (1986) classified the star as a cataclysmic variable, while Kilkenny et al. (1988) identified it as a sdB star. Reed et al. (2019) analyzed data collected during the *K2* mission and reported 46 frequencies in the p-mode region and 16 frequencies in the g-mode region. The g-modes are rather surprising at a high T_{eff} around 36 000 K. Among both p- and g-modes the authors identified consistent rotationally split frequencies and derived the rotation period of 16.18(57) days and concluded the star rotates as it were a solid body. The authors analyzed spectroscopic data reporting clear contribution from a main sequence companion. *TESS* observed the star during Sector 46. We detected just one frequency, which is the closest to f37 listed by Reed et al. (2019). This is surprising since we would expect the frequency were one of the highest amplitude in the *K2* data. It is then likely that the pulsation properties of this star changes significantly over a few years. We show an amplitude spectrum in Fig. 7, and we list the prewhitened frequencies in Table 4.

TIC 355058528 (Gaia DR3 6692773045444107008, V4640 Sgr, EC 20117-4014, CD-40 13747) is a known sdBV star. O'Donoghue et al. (1997) analyzed spectra and arrived at the conclusion that they are similar to spectra of other sdB stars. The authors also analyzed photometric time-series data and reported three frequencies, which were later confirmed, despite their effort, by Randall et al. (2006). The latter authors attempted a detailed asteroseismological analysis, arriving at two potential families of optimal models. *TESS* observed the star during Sector 27. We found only one frequency, which was reported by previous authors as the dominant amplitude one. We show an amplitude spectrum in Fig. 7, and we list the prewhitened frequencies in Table 4.

TIC 355638102 (Gaia DR3 6494992795056667648, EC 23507-5733, LB 1535) is a new sdOV star. Kilkenny et al. (2016) classified the star as He-sdO. *TESS* observed the star during Sector 28. We detected only two close frequencies. We show an amplitude spectrum in Fig. 7, and we list the prewhitened frequency in Table 4.

TIC 366399746 (Gaia DR3 601188910547673728) is a new sdBV star. The star has been classified as binary system consisting of sdB+MS by Luo et al. (2016). Sahoo et al. (2020a) reported one low frequencies and interpreted it as a binary signature. *TESS* observed the star during Sectors 45 and 46. We confirmed the low frequency, however it is of a very low amplitude. We detected one significant high frequency. We show an amplitude spectrum in Fig. 7, and we list the prewhitened frequency in Table 4.

TIC 396954061 (Gaia DR3 3259060049366022400, 2M 0415+0154) is a known sdBV star. Oreiro et al. (2009) analyzed spectra and derived T_{eff} and log g characteristic of sdB stars. The authors also analyzed time-series data and reported three frequencies. *TESS* observed the star during Sector 32. We confirm f_1 listed by Oreiro et al. (2009), while the other two we found different by a few μHz. These two frequencies are close to each other and could have not been resolved well in the run obtained by Oreiro et al. (2009). We show an amplitude spectrum in Fig. 9, and we list the prewhitened frequencies in Table 4.

TIC 409644971 (Gaia DR3 5947131955116293760) is a new sdBV star. Németh et al. (2012) analyzed the star spectroscopically and concluded it is a binary system consisting of a sdB and a F7 main sequence component. *TESS* observed the star during Sector 39. The light curve shows a reflection effect with a period of 0.09 day and we show the phase folded data in Fig. 8, while the ephemeris is provided in Table 3. The binary frequency and its three harmonics, as a consequence of a non sinusoidal shape of a flux variation, are listed in Table 4. In addition to the binary frequencies, we detected 10 frequencies in the high frequency region, which we associate with p-modes. We show an amplitude spectrum in Fig. 9.

TIC 434923593 (Gaia DR3 5862700251105587968, CS 1246) is a known sdBV star. Barlow et al. (2010) confirmed the sdB type and reported on their analysis of photometric data and a discovery listing one high amplitude frequency detected. *TESS* observed the star during Sector 38. We detected one high frequency with an amplitude of 10.6 ppt, which is substantially lower than during its discovery. We show an amplitude spectrum in Fig. 9, and we list the prewhitened frequency in Table 4.

TIC 436579904 (Gaia DR3 3308791681845675136, V1405 Ori, KUV 04421+1416) is a known sdBV star. Kilkenny et al. (1988) classified the star as sdB. Koen et al. (1999) analyzed time-series data and reported seven frequencies. The authors noticed the star to be noticeably red and expected it to be a binary, however no Ca II K line or a G band was detected. Reed et al. (2020) reported on their analyses of *K2* data. The authors detected a flux variation caused by binarity, confirming the suspicion of Koen et al. (1999). The flux variation is caused by the so-called reflection effect and the orbital period equals 0.398 day. Reed et al. (2020) listed 107 high frequencies attributed to p-modes. Some of the frequencies were explained by rotationally split multiplets. Additional 19 frequencies were detected in the low frequency region and attributed to g-modes. The authors used an asymptotic period spacing to identify the modal degree. *TESS* observed the star during Sectors 32, 43 and 44. The phase folded light curve showing the reflection effect is presented in Fig. 10, while the ephemeris is provided in Table 3. First, we calculated amplitude spectra from single sector data. In each spectrum we detected a handful of high frequencies, however they vary significantly between sectors and therefore we decided to analyze the sector data separately. We show an amplitude spectrum calculated only from Sector 44 data in Fig. 9, and we list the prewhitened frequencies in Table 4.

TIC 437043466 (Gaia DR3 6115879197240273 92, GALEX J085649.3+170115, EPIC 211779126) is a known sdBV star. It was identified as an sdB star by Németh et al. (2012). Pulsations were found by Baran et al. (2017). The authors reported the results of their analysis of the *K2* data. They found 154 frequencies in the g-mode and 29 in the p-mode regions, which makes the star a hybrid pulsator. Rotationally split modes allowed for estimation of a rotation rate to be ~16 days. Trapped modes were also reported. *TESS* observed the star during Sectors 44, 45 and 46. First, we compared the amplitude spectra calculated from single sector data. We detected two frequencies in the p-mode region in all sectors, which are the highest amplitude frequencies found by Baran et al. (2017). The g-mode region looks differently, however the majority of frequencies repeat. When we combined all sector data together

Table 4: List of frequencies we detected in the targets observed in the USC.

ID	Frequency [μHz]	Period [sec]	Amplitude [ppt]	S/N
		TIC 29840077		
f_1	2773.435(35)	360.5638(45)	6.4(9)	6.3
f_2	3100.724(40)	322.5053(41)	5.5(9)	5.5
		TIC 33318760		
f_1	811.098(43)	1232.90(7)	3.1(6)	4.7
f_2	7237.321(41)	138.1727(8)	3.3(6)	4.9
f_3	7353.243(37)	135.9944(7)	3.6(6)	5.4
		TIC 47377536 - Sector 35		
f_1	6177.659(7)	161.87361(19)	4.95(15)	28.3
f_2	6887.052(8)	145.20002(17)	4.37(15)	25.1
f_3	7038.032(5)	142.08518(11)	6.83(15)	39.1
f_4	7039.220(44)	142.0612(9)	0.93(16)	5.3
f_5	7040.235(10)	142.04072(21)	3.86(16)	22.1
f_6	7502.355(35)	133.2915(6)	1.02(15)	5.8
f_7	8927.686(42)	112.0111(5)	0.84(15)	4.8
f_8	9601.223(21)	104.15340(23)	1.65(15)	9.5
		TIC 47377536 - Sector 46		
f_1	6126.410(43)	163.2277(11)	0.71(13)	4.7
f_2	6177.671(8)	161.87329(21)	3.77(13)	25.3
f_3	6886.989(14)	145.20133(30)	2.14(13)	14.4
f_4	7015.248(12)	142.54664(24)	2.61(13)	17.5
f_5	7023.160(26)	142.3860(5)	1.17(13)	7.8
f_6	7037.903(7)	142.08779(15)	4.35(13)	29.1
f_7	7039.235(30)	142.0609(6)	1.12(13)	7.5
f_8	7040.267(25)	142.0401(5)	1.30(13)	8.7
f_9	9601.799(35)	104.14715(38)	0.88(13)	5.9
f_{10}	9605.438(33)	104.10769(35)	0.94(13)	6.3
		TIC 53826859		
f_1	2105.858(27)	474.866(6)	2.70(30)	7.5
f_2	2128.491(42)	469.816(9)	1.72(30)	4.8
f_3	2250.146(46)	444.416(9)	1.59(30)	4.4
f_4	2288.961(20)	436.8795(38)	3.63(30)	10.1
f_5	2296.4226(28)	435.4599(5)	26.36(30)	73.5
f_6	2378.113(7)	420.5015(12)	10.88(31)	30.3
f_7	2379.305(39)	420.291(7)	1.92(31)	5.3
f_8	2391.743(28)	418.1050(48)	2.63(30)	7.3
f_9	2404.780(43)	415.838(7)	1.74(30)	4.9
f_{10}	2405.740(13)	415.6725(22)	5.89(30)	16.4
f_{11}	2915.990(30)	342.9368(35)	2.41(30)	6.7
		TIC 60257911		
f_1	6851.861(10)	145.94575(21)	1.71(21)	7.0
f_2	7132.154(8)	140.21011(17)	1.97(21)	8.0
		TIC 62381958		
f_1	474.540(36)	2107.31(16)	0.300(46)	5.5
f_2	6781.622(40)	147.4573(9)	0.270(46)	5.0
f_3	6857.670(34)	145.8221(7)	0.34(5)	6.3
f_4	6858.271(26)	145.8093(6)	0.69(6)	12.6
f_5	6858.946(12)	145.79500(25)	2.05(6)	37.7
f_6	6859.480(16)	145.78365(34)	1.12(6)	20.7
f_7	7117.3685(13)	140.501366(26)	8.092(46)	149.0
f_8	7865.906(20)	127.13093(32)	0.542(46)	10.0
f_9	7872.533(9)	127.02392(14)	2.056(50)	37.9
f_{10}	7873.061(17)	127.01540(27)	1.01(6)	18.6
f_{11}	7873.496(47)	127.0084(8)	0.46(5)	8.6
f_{12}	8128.686(33)	123.0211(5)	0.322(47)	5.9
f_{13}	8132.647(42)	122.9612(6)	0.256(47)	4.7
f_{14}	8248.532(18)	121.23370(27)	0.614(48)	11.3

Table 4: continued.

ID	Frequency [μHz]	Period [sec]	Amplitude [ppt]	S/N
f_{15}	8250.215(14)	121.20897(21)	0.792(48)	14.6
f_{16}	8253.728(26)	121.15738(38)	0.433(48)	8.0
f_{17}	8255.212(19)	121.13559(27)	0.599(48)	11.0
f_{18}	8257.489(31)	121.10219(45)	0.354(47)	6.5
f_{19}	8313.416(33)	120.28749(48)	0.324(47)	6.0
f_{20}	8315.952(38)	120.2508(5)	0.285(47)	5.3
f_{21}	8538.002(39)	117.1234(5)	0.280(46)	5.2
f_{22}	8551.761(28)	116.93498(39)	0.394(47)	7.3
f_{23}	8553.080(22)	116.91694(30)	0.539(47)	9.9
f_{24}	8554.252(31)	116.90093(43)	0.372(47)	6.9
f_{25}	8582.687(36)	116.51363(49)	0.301(46)	5.5
f_{26}	9075.155(41)	110.19095(50)	0.329(47)	6.1
f_{27}	9075.611(37)	110.18542(45)	0.361(47)	6.6
f_{28}	9248.504(17)	108.12559(19)	0.649(46)	11.9
f_{29}	10104.297(24)	98.96780(23)	0.457(46)	8.4
f_{30}	10109.795(11)	98.91397(11)	0.941(46)	17.3
f_{31}	11013.191(27)	90.80021(23)	0.405(47)	7.5
f_{32}	11014.243(27)	90.79154(23)	0.42(5)	7.8
f_{33}	11015.080(25)	90.78464(21)	0.46(5)	8.4
f_{34}	11548.886(33)	86.58844(25)	0.331(47)	6.1
f_{35}	11550.280(30)	86.57799(23)	0.362(47)	6.7
f_{36}	11555.972(35)	86.53535(26)	0.305(46)	5.6
f_{37}	12732.841(35)	78.53707(22)	0.31(5)	5.8
f_{38}	12733.566(32)	78.53260(19)	0.35(5)	6.4
		TIC 62483415		
f_1	5679.263(6)	176.07920(18)	7.09(15)	39.0
f_2	6361.145(8)	157.20441(19)	5.36(15)	29.5
f_3	7355.040(21)	135.96119(39)	1.92(15)	10.6
f_4	7994.651(47)	125.0836(7)	0.87(15)	4.8
f_5	8112.27	123.27	2.13	11.7
f_6	8423.390(9)	118.71705(13)	4.44(15)	24.4
f_7	8771.747(31)	114.00238(40)	1.31(16)	7.2
f_8	8774.283(29)	113.96943(38)	1.39(16)	7.6
f_9	9335.296(42)	107.12033(48)	0.96(15)	5.3
f_{10}	10414.542(31)	96.01959(28)	1.32(15)	7.2
f_{11}	11358.495(47)	88.03983(36)	0.86(15)	4.7
f_{12}	12040.401(32)	83.05371(22)	1.27(15)	7.0
		TIC 69298924		
f_1	2612.210(10)	382.8176(15)	1.53(20)	6.5
f_2	2817.4790(47)	354.9272(6)	3.49(21)	14.7
f_3	2818.3782(12)	354.81399(15)	13.44(21)	56.7
f_4	2819.2695(44)	354.7018(6)	3.69(21)	15.6
		TIC 70549283		
f_1	7365.283(7)	135.77210(13)	7.1(6)	9.7
		TIC 98871628		
f_1	6717.023(34)	148.8755(8)	1.23(16)	6.4
		TIC 139723188		
f_1	6563.105(23)	152.3669(5)	2.48(45)	4.7
f_2	7110.363(6)	140.63979(11)	9.91(45)	18.9
f_3	7769.015(10)	128.71644(16)	5.70(45)	10.9
		TIC 156618553		
f_1	140.886(22)	7097.9(1.1)	0.209(19)	9.3
f_2	152.895(30)	6540.4(1.3)	0.153(19)	6.8
f_3	168.189(32)	5945.7(1.1)	0.144(19)	6.4
f_4	3074.053(42)	325.3034(45)	0.108(19)	4.8
		TIC 169285097		
f_1	86.517(35)	11558.4(4.7)	0.149(22)	5.8
f_2	100.4796(29)	9952.27(29)	1.822(22)	71.6
f_3	112.741(13)	8869.9(10)	0.419(22)	16.5

Table 4: continued.

ID	Frequency [μHz]	Period [sec]	Amplitude [ppt]	S/N
f_4	128.521(21)	7780.8(1.3)	0.251(22)	9.8
f_5	131.818(33)	7586.2(1.9)	0.159(22)	6.2
f_6	136.892(15)	7305.0(8)	0.363(22)	14.2
f_7	142.904(19)	6997.7(9)	0.278(22)	10.9
f_8	151.956(20)	6580.9(9)	0.272(22)	10.7
f_9	153.936(41)	6496.2(1.7)	0.133(22)	5.2
f_{10}	160.390(43)	6234.8(1.7)	0.122(22)	4.8
f_{11}	165.230(14)	6052.2(5)	0.384(22)	15.1
f_{12}	174.943(38)	5716.2(1.2)	0.140(22)	5.5
f_{13}	182.595(36)	5476.6(1.1)	0.148(22)	5.8
f_{14}	202.204(49)	4945.5(1.2)	0.123(24)	4.8
f_{15}	202.950(47)	4927.3(1.1)	0.129(24)	5.1
f_{16}	213.913(17)	4674.80(38)	0.301(22)	11.8
f_{17}	236.868(11)	4221.75(19)	0.490(22)	19.2
f_{18}	246.254(41)	4060.8(7)	0.128(22)	5.0
f_{19}	255.875(20)	3908.16(31)	0.261(22)	10.2
f_{20}	258.1895(33)	3873.125(50)	1.596(22)	62.6
f_{21}	266.352(26)	3754.42(36)	0.206(22)	8.1
f_{22}	273.520(5)	3656.04(7)	0.963(22)	37.8
f_{23}	279.755(12)	3574.56(15)	0.454(22)	17.8
f_{24}	285.358(39)	3504.37(48)	0.135(22)	5.3
f_{25}	289.801(10)	3450.64(12)	0.543(22)	21.3
f_{26}	302.880(10)	3301.64(11)	0.523(22)	20.6
f_{27}	330.554(10)	3025.23(9)	0.542(22)	21.3
f_{28}	621.311(36)	1609.50(9)	0.144(22)	5.7
f_{29}	670.248(33)	1491.98(7)	0.158(22)	6.2
f_{30}	2582.8748(38)	387.1655(6)	1.395(22)	54.8
f_{31}	2793.919(5)	357.9202(7)	0.990(22)	38.9
f_{32}	2808.268(21)	356.0914(27)	0.247(22)	9.7
f_{33}	2837.274(39)	352.4510(49)	0.133(22)	5.2
f_{34}	3736.793(25)	267.6091(18)	0.210(22)	8.2
TIC 220573709 - Sector 28				
f_1	12.101(9)	82639(64)	7.95(29)	23.0
f_2	29249.216(38)	34.188950(44)	1.98(29)	5.7
f_3	29260.736(45)	34.17549(5)	1.65(29)	4.8
f_4	32110.695(46)	31.142272(45)	1.61(29)	4.7
f_5	32122.806(37)	31.130531(35)	2.03(29)	5.9
TIC 220573709 - Sector 30				
f_1	12.117(9)	82525(58)	7.50(27)	23.1
f_2	32110.729(36)	31.142239(35)	1.77(28)	5.5
f_3	32122.803(26)	31.130534(25)	2.48(28)	7.6
f_4	32134.910(34)	31.118805(33)	1.88(28)	5.8
TIC 241771689				
f_1	259.786(34)	3849.3(5)	0.308(45)	6.1
f_2	287.564(33)	3477.49(40)	0.322(45)	6.4
f_3	387.329(20)	2581.78(13)	0.536(45)	10.7
f_4	407.599(32)	2453.39(19)	0.333(45)	6.6
f_5	487.487(26)	2051.34(11)	0.408(45)	8.2
f_6	527.160(35)	1896.96(13)	0.300(45)	6.0
f_7	5083.355(7)	196.72047(26)	1.648(45)	32.9
f_8	5084.558(9)	196.67395(33)	1.278(46)	25.5
f_9	5086.1950(42)	196.61063(16)	2.634(46)	52.6
f_{10}	5087.4084(15)	196.56374(6)	7.313(46)	146.1
f_{11}	5088.687(12)	196.51434(45)	0.942(46)	18.8
f_{12}	5103.4866(45)	195.94447(17)	2.378(46)	47.5
f_{13}	5104.781(15)	195.8948(6)	0.725(46)	14.5
f_{14}	5108.834(20)	195.7394(8)	0.534(45)	10.7
f_{15}	5120.9515(9)	195.276209(33)	12.556(45)	250.8
f_{16}	5122.4560(21)	195.21886(8)	5.274(45)	105.4

Table 4: continued.

ID	Frequency [μHz]	Period [sec]	Amplitude [ppt]	S/N
f_{17}	5161.239(34)	193.7519(13)	0.315(46)	6.3
f_{18}	5162.894(22)	193.6898(8)	0.488(46)	9.8
f_{19}	5164.558(16)	193.6274(6)	0.671(46)	13.4
f_{20}	5167.806(30)	193.5057(11)	0.377(46)	7.5
f_{21}	5169.337(17)	193.4484(6)	0.666(46)	13.3
f_{22}	5170.994(13)	193.38640(48)	0.850(46)	17.0
f_{23}	5172.420(25)	193.3331(9)	0.431(46)	8.6
f_{24}	5511.071(26)	181.4529(9)	0.409(45)	8.2
f_{25}	5512.663(42)	181.4005(14)	0.254(45)	5.1
f_{26}	6483.865(14)	154.22900(32)	0.776(45)	15.5
f_{27}	6684.175(26)	149.6071(6)	0.413(45)	8.2
f_{28}	6698.453(29)	149.2882(6)	0.368(45)	7.3
f_{29}	6955.703(38)	143.7669(8)	0.277(45)	5.5
f_{30}	6984.463(7)	143.17492(15)	1.476(45)	29.5
f_{31}	6987.269(7)	143.11742(13)	1.613(45)	32.2
f_{32}	7232.792(27)	138.2592(5)	0.398(45)	7.9
f_{33}	7234.885(14)	138.21920(27)	0.759(45)	15.2
f_{34}	7240.332(18)	138.11521(35)	0.574(45)	11.5
f_{35}	7337.163(23)	136.29246(43)	0.460(45)	9.2
f_{36}	7866.582(24)	127.12001(38)	0.444(45)	8.9
f_{37}	8610.425(27)	116.13829(37)	0.386(45)	7.7
f_{38}	10170.809(27)	98.32060(26)	0.395(45)	7.9
f_{39}	10205.803(21)	97.98347(20)	0.533(46)	10.6
f_{40}	10207.182(31)	97.97023(30)	0.358(46)	7.1
f_{41}	10208.452(31)	97.95805(30)	0.344(45)	6.9
f_{42}	10241.876(38)	97.63836(36)	0.282(45)	5.6
		TIC 248949857		
f_1	7452.395(13)	134.18506(24)	0.644(37)	15.0
f_2	7454.121(25)	134.15398(44)	0.344(37)	8.0
f_3	7866.851(19)	127.11567(31)	0.436(37)	10.1
f_4	7867.927(16)	127.09829(25)	0.542(37)	12.6
f_5	7872.224(18)	127.02891(30)	0.460(37)	10.7
f_6	8087.273(37)	123.6511(6)	0.227(37)	5.3
f_7	8090.699(39)	123.5987(6)	0.216(37)	5.0
f_8	8091.851(9)	123.58112(13)	0.979(37)	22.8
f_9	8150.510(6)	122.69170(10)	1.382(38)	32.1
f_{10}	8151.414(21)	122.67810(31)	0.431(38)	10.0
f_{11}	10621.750(27)	94.14645(24)	0.307(37)	7.1
		TIC 273218137		
f_{bin}	2.0259(38)	493618(918)	8.38(13)	57.8
f_1	194.302(37)	5146.6(10)	0.85(13)	5.9
f_2	310.612(39)	3219.45(41)	0.80(13)	5.5
f_3	314.259(38)	3182.09(38)	0.83(13)	5.7
f_4	2923.083(15)	342.1045(18)	2.05(13)	14.1
f_5	2926.7716(14)	341.67340(17)	21.90(13)	151.0
f_6	2930.474(14)	341.2417(16)	2.32(13)	16.0
$2f_5$	5853.5432	170.83670	0.75(13)	5.2
		TIC 322009509		
f_1	6867.122(39)	145.6214(8)	2.67(43)	5.3
f_2	7092.261(22)	140.99875(45)	4.63(43)	9.2
		TIC 335635628		
f_1	8436.512(17)	118.53240(24)	6.63(48)	11.8
		TIC 355058528		
f_1	7284.618(17)	137.27555(32)	1.07(7)	13.1
		TIC 355638102		
f_1	9214.066(32)	108.52972(38)	8.1(1.0)	6.9
f_2	9217.449(45)	108.4899(5)	5.9(1.0)	5.0
		TIC 366399746		
f_1	6890.6238(42)	145.12474(9)	5.40(19)	23.7

Table 4: continued.

ID	Frequency [μHz]	Period [sec]	Amplitude [ppt]	S/N
TIC 396954061				
f_1	6707.801(23)	149.0802(5)	1.88(18)	8.9
f_2	6710.727(23)	149.0151(5)	1.83(18)	8.7
f_3	6949.580(6)	143.89359(13)	6.82(18)	32.3
TIC 409644971				
f_{orb}	127.55181(38)	7839.951(24)	39.46(7)	515.1
$2f_{orb}$	255.10363	3919.976	4.28(7)	55.9
$3f_{orb}$	382.65544	2613.317	0.37(7)	4.8
$4f_{orb}$	510.20726	1959.988	0.50(7)	6.6
f_1	5576.723(39)	179.3168(12)	0.40(7)	5.2
f_2	5618.818(24)	177.9734(8)	0.64(7)	8.4
f_3	5721.991(40)	174.7643(12)	0.38(7)	5.0
f_4	5768.337(24)	173.3602(7)	0.64(7)	8.3
f_5	5849.489(37)	170.9551(11)	0.42(7)	5.5
f_6	5873.919(23)	170.2441(7)	0.69(7)	9.0
f_7	5899.028(41)	169.5194(12)	0.37(7)	4.9
f_8	6060.126(27)	165.0131(7)	0.57(7)	7.4
f_9	6154.086(25)	162.4937(7)	0.62(7)	8.1
f_{10}	6597.850(32)	151.5645(7)	0.48(7)	6.3
TIC 434923593				
f_1	2690.419(15)	371.6893(21)	10.6(7)	13.0
TIC 436579904 - Sector 32				
f_{bin}	29.0787(7)	34389.4(8)	102.10(33)	267.4
$2f_{bin}$	58.157410	17194.713533	18.47(33)	48.4
f_1	4324.405(34)	231.2457(18)	2.24(33)	5.9
f_2	4340.964(21)	230.3636(11)	3.63(33)	9.5
f_3	4621.220(21)	216.3931(10)	3.61(33)	9.4
f_4	4645.398(45)	215.2668(21)	1.72(33)	4.5
f_5	4654.887(26)	214.8280(12)	2.94(33)	7.7
f_6	4703.585(17)	212.6038(8)	4.47(33)	11.7
TIC 436579904 - Sector 43				
f_{bin}	29.0811(8)	34386.6(9)	97.99(33)	253.7
$2f_{bin}$	58.162137	17193.316114	18.68(33)	48.4
f_1	4324.383(33)	231.2468(18)	2.48(33)	6.4
f_2	4341.029(22)	230.3602(12)	3.72(33)	9.6
f_3	4610.302(33)	216.9055(15)	2.51(33)	6.5
f_4	4618.258(49)	216.5319(23)	1.68(33)	4.3
f_5	4621.284(24)	216.3901(11)	3.46(33)	9.0
f_6	4703.576(30)	212.6042(14)	2.72(33)	7.0
TIC 436579904 - Sector 44				
f_{bin}	29.0801(7)	34387.8(8)	110.97(31)	304.8
$2f_{bin}$	58.160185	17193.892984	21.36(31)	58.7
f_1	4247.838(47)	235.4139(26)	1.70(31)	4.7
f_2	4324.387(29)	231.2467(15)	2.75(31)	7.6
f_3	4340.972(22)	230.3632(12)	3.64(31)	10.0
f_4	4610.331(24)	216.9042(11)	3.35(31)	9.2
f_5	4621.284(19)	216.3901(9)	4.10(31)	11.3
f_6	4640.524(41)	215.4929(19)	1.95(31)	5.4
f_7	4655.098(25)	214.8182(12)	3.16(31)	8.7
f_8	4683.284(42)	213.5254(19)	1.92(31)	5.3
f_9	4703.663(35)	212.6003(16)	2.28(31)	6.3
TIC 437043466 - Sector 44				
f_1	116.547(44)	8580.2(3.2)	0.54(9)	4.9
f_2	152.365(25)	6563.2(1.1)	0.93(9)	8.4
f_3	158.935(38)	6291.9(1.5)	0.63(9)	5.7
f_4	220.493(42)	4535.3(9)	0.57(9)	5.1
f_5	287.124(34)	3482.82(41)	0.70(9)	6.3
f_6	2544.276(38)	393.039(6)	0.62(9)	5.6
f_7	2739.119(26)	365.0809(34)	0.92(9)	8.3

we detected all but one frequency (f_3 in Sector 45) we detected in single sector data, but on the other hand we detected two frequencies (f_6 and f_7 in Sectors 44-46), which are not significant in single sector data. In Table 4 we show all frequencies we found, while in Fig. 9 we show an amplitude spectra, both in single and merged-all sector data.

TIC 452718256 (Gaia DR3 3533727090595727104, EC 11275-2504) is a known sdOBV star. This star was classified as sdOB by Kilkenny et al. (1997b). Kilkenny et al. (2019) reported a discovery of a signal at frequencies around 6.78 mHz, and between 7.5 and 7.8 mHz, depending on data taken sporadically over 2 years. *TESS* observed the star during Sector 36. We detected two close frequencies around 6779 µHz. We show an amplitude spectrum in Fig. 9, and we list the prewhitened frequencies in Table 4.

TIC 471013461 (Gaia DR3 4843383737223292672, EC 03530-402) is a new sdBV star. Kilkenny et al. (2016) classified the star as sdB. *TESS* observed the star during Sector 1. We detected only one frequency in the p-mode region. We show an amplitude spectrum in Fig. 11, and we list the prewhitened frequency in Table 4.

TIC 673345538 (Gaia DR3 3296244226946647168, V1835 Ori) is a known sdBV star. Ramsay & Hakala (2005) found short period variability in the star, while Ramsay et al. (2006) identified the star as a sdB, while the flux variation was identified as p-mode pulsations. The low $T_{\rm eff}$ correlates with pulsation period below 3 000 µHz. Baran et al. (2011b) re-observed the star over the course of 47 days from two different sites and reported six frequencies in the g-mode region and six, including one combination, frequencies in the p-mode region. That discovery made the star a hybrid sdBV. *TESS* observed the star during Sector 43 and 44. We detected only one frequency, which is the highest amplitude frequency reported by Baran et al. (2011b). We show an amplitude spectrum in Fig. 11, and we list the prewhitened frequency in Table 4.

3.3. Other new variable stars

TIC 754255960 is located within the *TESS* target mask of TIC 1001123 and while checking on the contamination of this star we found the former to be a variable star, which shows two frequencies in an amplitude spectrum. Since the higher frequency is twice the lower frequency, we consider it to be a harmonic. We interpret such flux variation to be a consequence of a binarity. The orbital period equals 0.19942(6) days. We pulled out the light from the SC data and calculated the amplitude spectrum. Both plots are shown in Fig. 12.

TIC 434923595 and TIC 434925198 are located within the *TESS* target mask of TIC 434923593 and while checking on the contamination of this star we found the two former objects to be variable stars. We pulled out the light curves from the SC data and calculated the amplitude spectra. Plots of both stars are shown in Fig. 13 and 14.

Table 4: continued.

ID	Frequency [µHz]	Period [sec]	Amplitude [ppt]	S/N
TIC 437043466 - Sector 45				
f_1	116.201(47)	8605.7(3.5)	0.53(10)	4.7
f_2	152.422(31)	6560.7(1.3)	0.79(10)	7.1
f_3	172.896(38)	5783.8(1.3)	0.65(10)	5.8
f_4	287.122(29)	3482.84(35)	0.85(10)	7.6
f_5	2544.297(40)	393.036(6)	0.62(10)	5.5
f_6	2739.085(32)	365.0854(43)	0.77(10)	6.9
TIC 437043466 - Sector 46				
f_1	152.468(42)	6558.7(1.8)	0.48(9)	4.8
f_2	287.106(30)	3483.03(36)	0.68(9)	6.8
f_3	338.527(34)	2953.97(30)	0.59(9)	5.9
f_4	2544.289(44)	393.037(7)	0.47(9)	4.6
f_5	2739.159(37)	365.0756(50)	0.55(9)	5.4
TIC 437043466 - Sector 44-46				
f_1	116.278(14)	8600.0(1.0)	0.30(5)	4.8
f_2	152.252(13)	6568.1(6)	0.35(5)	5.7
f_3	152.410(7)	6561.24(29)	0.69(5)	11.1
f_4	158.947(9)	6291.40(35)	0.47(5)	7.6
f_5	220.572(10)	4533.68(20)	0.42(5)	6.8
f_6	249.124(11)	4014.06(18)	0.37(5)	5.9
f_7	266.452(11)	3753.02(15)	0.39(5)	6.2
f_8	287.132(6)	3482.72(7)	0.74(5)	11.9
f_9	327.673(15)	3051.82(14)	0.29(5)	4.6
f_{10}	338.620(10)	2953.16(9)	0.43(5)	6.9
f_{11}	2544.298(7)	393.0356(11)	0.57(5)	9.1
f_{12}	2739.133(6)	365.0790(8)	0.73(5)	11.8
TIC 452718256				
f_1	6779.306(33)	147.5077(7)	2.17(21)	9.9
f_2	6779.813(45)	147.4967(10)	1.59(21)	7.2
TIC 471013461				
f_1	2710.863(18)	368.8863(25)	12.9(10)	11.3
TIC 673345538				
f_1	2681.033(17)	372.9906(24)	16.1(2)	6.0

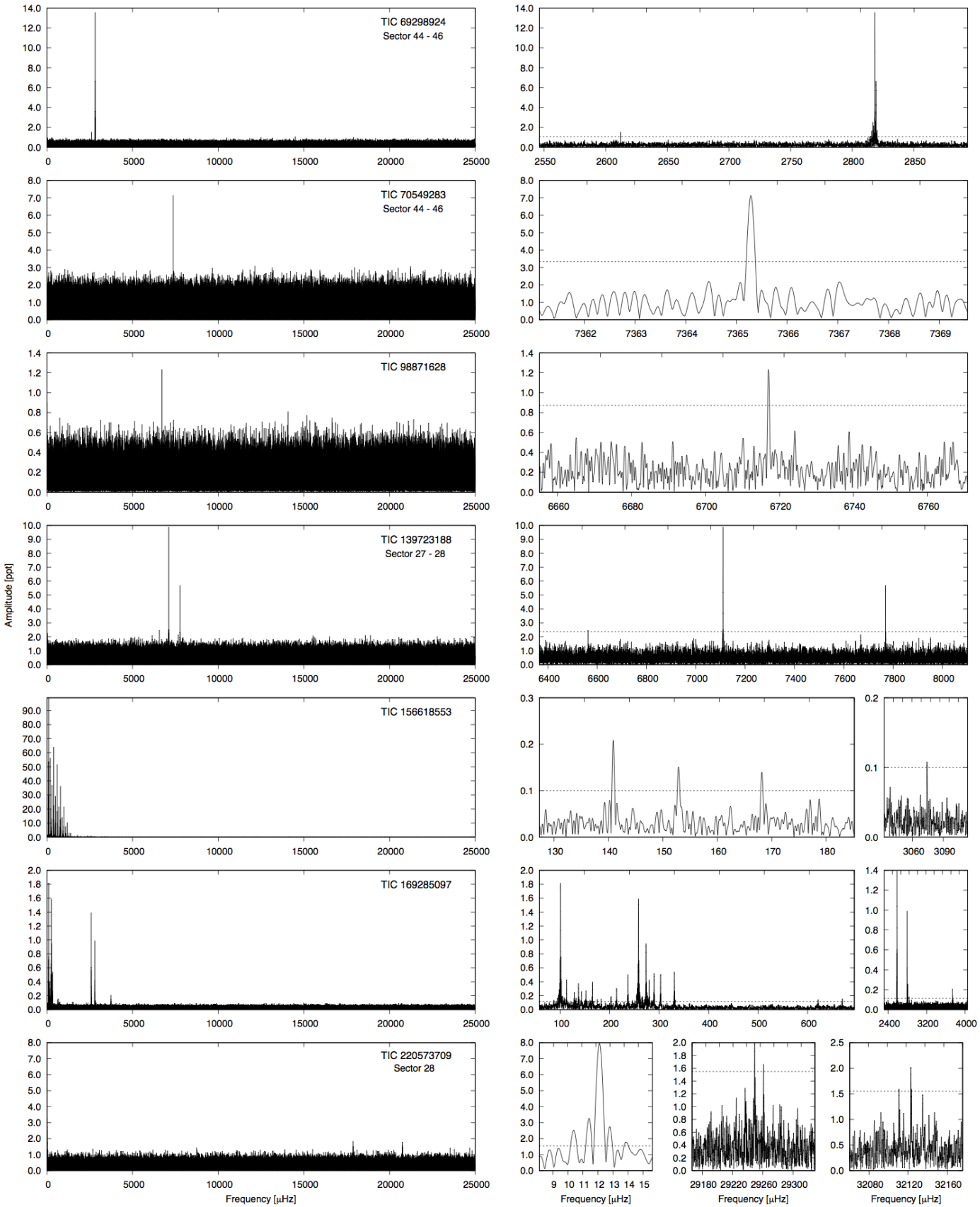

Fig. 6: Same as in Fig. 5 but for another seven targets observed in the USC.

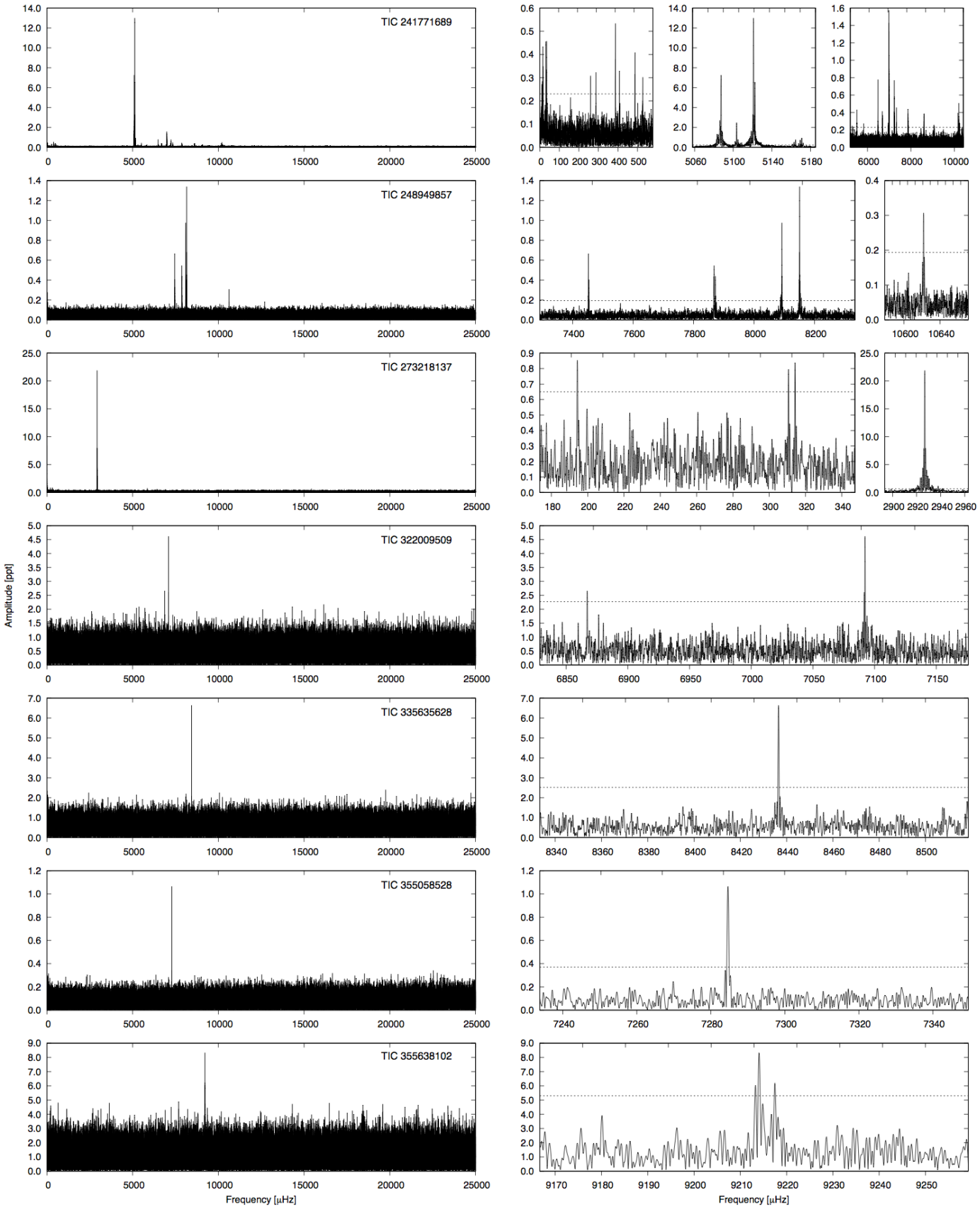

Fig. 7: Same as in Fig. 5 but for another seven targets observed in the USC.

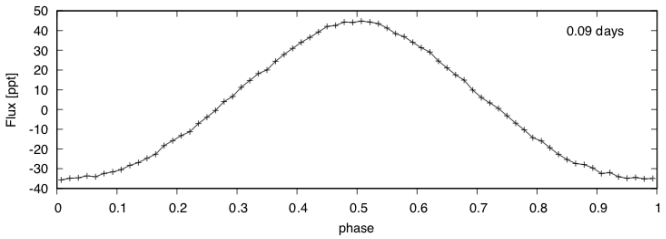

Fig. 8: Phase folded light curve of TIC 409644971 showing a reflection effect. The number in the upper right corner is the orbital period, rounded to two significant digits, used for folding the light curve.

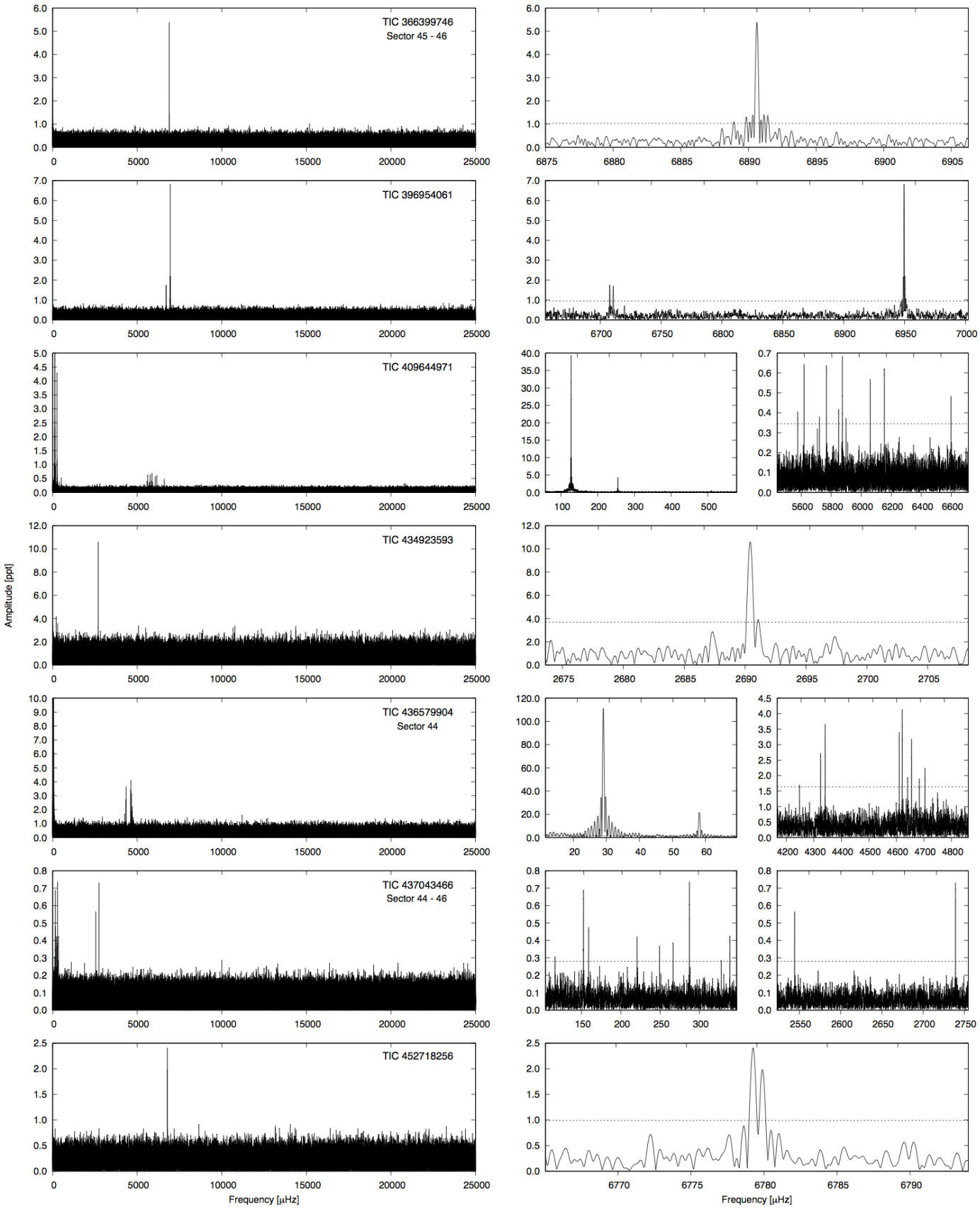

Fig. 9: Same as in Fig. 5 but for another seven targets observed in the USC.

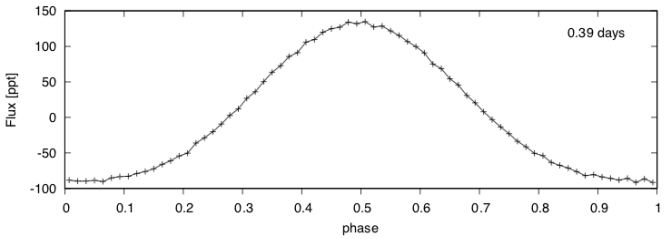

Fig. 10: Phase folded light curve of TIC 436579904 showing a reflection effect. The number in the upper right corner is the orbital period, rounded to two significant digits, used for folding the light curve.

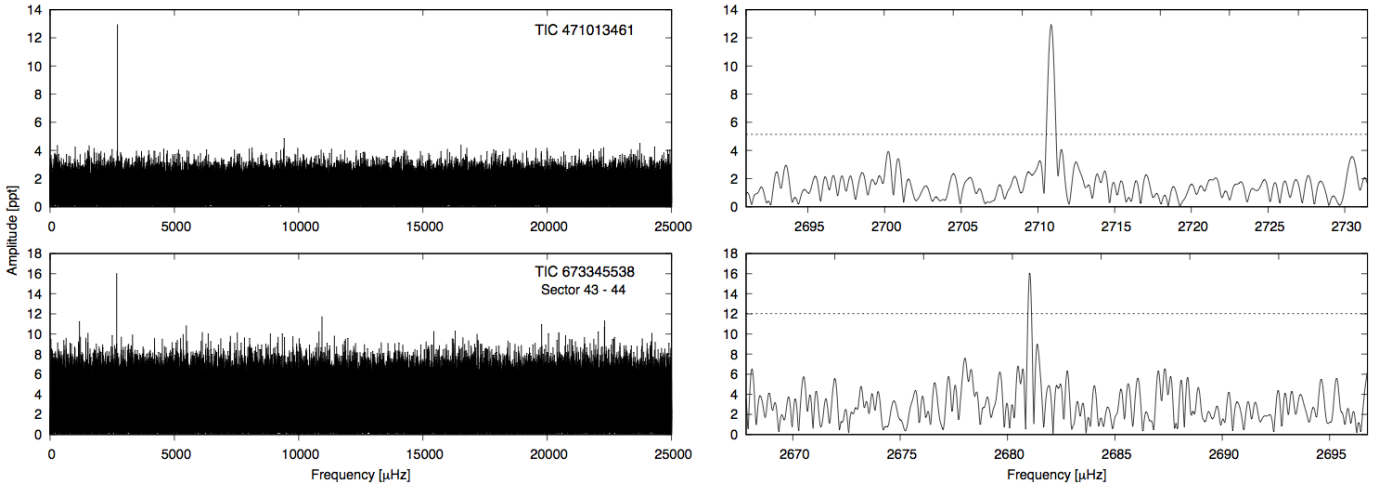

Fig. 11: Same as in Fig. 5 but for another two targets observed in the USC.

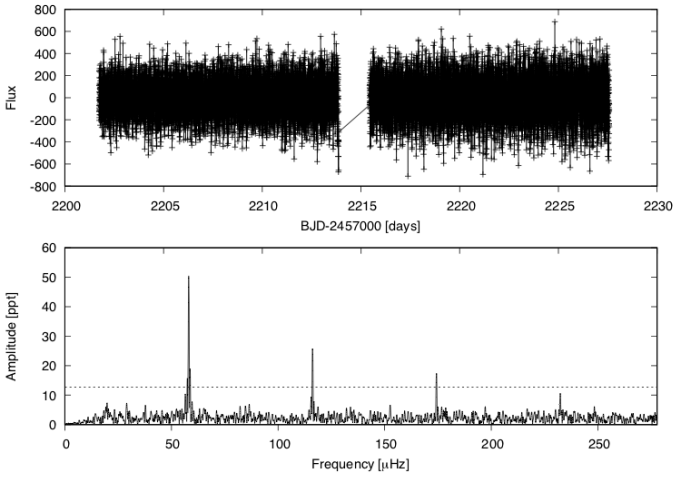

Fig. 12: *Top panel:* a light curve of TIC 754255960 derived from the Full Frame Images taken in Sector 33. *Bottom panel:* an amplitude spectrum calculated from the light curve sampled at 30 min. The horizontal line denotes the detection threshold at 4.5 times the median noise level in a residual amplitude spectrum (with two significant peaks removed).

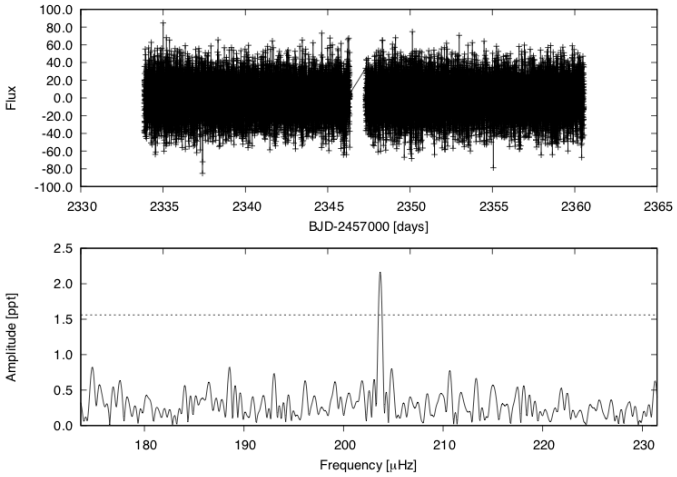

Fig. 13: Same as in Fig. 12 but of TIC 434923595 derived from the SC data taken during Sector 38.

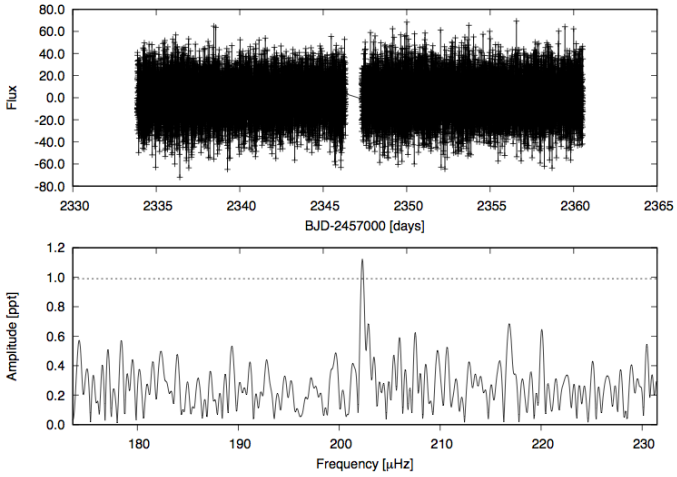

Fig. 14: Same as in Fig. 12 but of TIC 434925198 derived from the SC data taken during Sector 38.

4. Summary

We presented the result of our search for short period pulsating hot subdwarfs. We used *TESS* space data collected during Year 1 and 3 covering the Southern Ecliptic Hemisphere. We reported the stars that show signals at high frequencies associated with p-mode pulsations. In most cases the amplitudes of p-modes dominate amplitude spectra, however there are two stars that have gravity modes of comparable amplitudes. Except those two stars, 39 hot subdwarfs in our sample can be considered p-mode dominated pulsators.

While the majority of stars in our sample are sdB pulsators we found one new pulsator among sdO stars and two new pulsators among sdOB stars. Four pulsators are not discernible between sdB or sdOB and we temporarily classified them as sdBO.

We prewhitened frequencies above an assumed detection threshold. The number of frequencies detected in a given star varies from one to 42. Some stars show combination frequencies and or low frequencies along with harmonics. The latter is a typical signature of binarity. We identified three stars showing dominant, amplitude-wise, binary signatures and we phase the data to see the orbit variation. For TIC 156618553, which is a well known HW Vir-type prototype, we derived the mid-times of two *TESS*-orbit averaged eclipses.

We looked for multiplets that may help identifying geometry of the modes and estimating rotation periods of those pulsators. Out of 41 targets only for five known pulsators, multiplets were reported. These are TIC 47377536, TIC 60257911, TIC 62483415, TIC 335635628 and TIC 437043466. We confirm none of those multiplets. In five cases, three new (TIC 139481265, TIC 241771689 and TIC 273218137) and two known (TIC 69298924 and TIC 220573709) pulsators, we found candidates for rotationally split frequencies, however this detection should be confirmed with longer data coverage. The estimated rotation periods range between 0.7 and 12.9 d.

Besides the primary goal of this paper, we also found three other new variables, which happened to be accidentally located in the target masks of two of our program targets. We detected these stars while doing contamination analysis to avoid false positives. The frequencies detected in TIC 434925198 and TIC 434923595 is only marginally above the detection threshold, while the signal in TIC 754255960 is quite significant. The latter shows three harmonics indicating a non-sinusoidal shape of a flux variation. This can be interpreted as shallow eclipses but there are also other explanations. The spectroscopic observations are advised to classify variability types of these three new variables.

Acknowledgements. Financial support from the National Science Centre in Poland under project No. UMO-2017/26/E/ST9/00703 is acknowledged. This paper includes data collected with the *TESS* mission, obtained from the MAST data archive at the Space Telescope Science Institute (STScI). Funding for the *TESS* mission is provided by the NASA Explorer Program. STScI is operated by the Association of Universities for Research in Astronomy, Inc., under NASA contract NAS 5–26555. This paper uses observations made at the South African Astronomical Observatory (SAAO). This research has made use of the SIMBAD database, operated at CDS, Strasbourg, France. This work has also made use of data from the European Space Agency (ESA) mission *Gaia* (https://www.cosmos.esa.int/gaia), processed by the *Gaia* Data Processing and Analysis Consortium (DPAC, https://www.cosmos.esa.int/web/gaia/dpac/consortium). Funding for the DPAC has been provided by national institutions, in particular the institutions participating in the *Gaia* Multilateral Agreement. V.V.G. is a F.R.S.-FNRS Research Associate.

References

Baran, A., Oreiro, R., Pigulski, A., et al. 2009, MNRAS, 392, 1092
Baran, A., Østensen, R., Telting, J., et al. 2018, MNRAS, 481, 2721
Baran, A., Pigulski, A., Kozieł, D., et al. 2005, MNRAS, 360, 737
Baran, A. S., Gilker, J. T., Fox-Machado, L., Reed, M. D., & Kawaler, S. D. 2011b, MNRAS, 411, 776
Baran, A. S., Gilker, J. T., Reed, M. D., et al. 2011a, MNRAS, 413, 2838
Baran, A. S. & Koen, C. 2021, Acta Astron., 71, 113
Baran, A. S., Reed, M. D., Østensen, R. H., Telting, J. H., & Jeffery, C. S. 2017, A&A, 597, A95
Baran, A. S., Reed, M. D., Stello, D., et al. 2012, MNRAS, 424, 2686
Barlow, B. N., Dunlap, B. H., Clemens, J. C., et al. 2010, MNRAS, 403, 324
Barlow, B. N., Dunlap, B. H., Lynas-Gray, A. E., & Clemens, J. C. 2009, AJ, 138, 686
Barlow, B. N., Kilkenny, D., Geier, S., et al. 2017, PASP, 129, 054202
Beers, T. C., Preston, G. W., Shectman, S. A., Doinidis, S. P., & Griffin, K. E. 1992, AJ, 103, 267
Berger, J. & Fringant, A. M. 1980, A&A, 85, 367
Billères, M., Fontaine, G., Brassard, P., et al. 1997, ApJ, 487, L81
Charpinet, S., Fontaine, G., & Brassard, P. 2003, in NATO Advanced Study Institute (ASI) Series B, Vol. 105, White Dwarfs, 69
Charpinet, S., Fontaine, G., Brassard, P., et al. 1997, ApJ, 483, 123
Charpinet, S., Green, E. M., Baglin, A., et al. 2010, A&A, 516, L6
Edelmann, H., Heber, U., Altmann, M., Karl, C., & Lisker, T. 2005, A&A, 442, 1023
Fontaine, G., Brassard, P., Charpinet, S., et al. 2012, A&A, 539, 12
Fontaine, G., Brassard, P., Green, E. M., et al. 2008, A&A, 486, L39
Geier, S. 2013, A&A, 549, 110
Green, E. M., Fontaine, G., Reed, M. D., et al. 2003, ApJ, 583, 31
Green, R. F., Schmidt, M., & Liebert, J. 1986, ApJS, 61, 305
Han, Z., Podsiadlowski, P., Maxted, P. F. L., Marsh, T. R., & Ivanova, N. 2002, MNRAS, 336, 449
Iben, I., J. & Tutukov, A. V. 1984, ApJS, 54, 335
Iben, Icko, J. 1990, ApJ, 353, 215
Johnson, C., Green, E., Wallace, S., et al. 2014, in Astronomical Society of the Pacific Conference Series, Vol. 481, 6th Meeting on Hot Subdwarf Stars and Related Objects, ed. V. van Grootel, E. Green, G. Fontaine, & S. Charpinet, 153
Kawka, A., Vennes, S., O'Toole, S., et al. 2015, MNRAS, 450, 3514
Kawka, A., Vennes, S., Schmidt, G. D., Wickramasinghe, D. T., & Koch, R. 2007, ApJ, 654, 499
Kilkenny, D. 1987, MNRAS, 228, 713
Kilkenny, D., Billères, M., Stobie, R. S., et al. 2002, MNRAS, 331, 399
Kilkenny, D., Heber, U., & Drilling, J. S. 1988, South African Astronomical Observatory Circular, 12, 1
Kilkenny, D., Koen, C., O'Donoghue, D., & Stobie, R. S. 1997a, MNRAS, 285, 640
Kilkenny, D., Koen, C., & Worters, H. 2010, MNRAS, 404, 376
Kilkenny, D., O'Donoghue, D., Crause, L., et al. 2009, MNRAS, 396, 548
Kilkenny, D., O'Donoghue, D., Koen, C., Stobie, R. S., & Chen, A. 1997b, MNRAS, 287, 867
Kilkenny, D., O'Donoghue, D., Worters, H. L., et al. 2015, MNRAS, 453, 1879
Kilkenny, D., Stobie, R. S., O'Donoghue, D., et al. 2006, MNRAS, 367, 1603
Kilkenny, D., Worters, H. L., & Lynas-Gray, A. E. 2019, MNRAS, 485, 4330
Kilkenny, D., Worters, H. L., O'Donoghue, D., et al. 2016, MNRAS, 459, 4343
Kilkenny, D., Worters, H. L., & Østensen, R. H. 2017a, MNRAS, 467, 3963
Kilkenny, D., Worters, H. L., & Østensen, R. H. 2017b, MNRAS, 467, 3963
Koen, C. 2007, MNRAS, 377, 1275
Koen, C., Kilkenny, D., O'Donoghue, D., van Wyk, F., & Stobie, R. S. 1997, MNRAS, 285, 645
Koen, C., O'Donoghue, D., Kilkenny, D., Stobie, R. S., & Saffer, R. A. 1999, MNRAS, 306, 213
Lamontagne, R., Demers, S., Wesemael, F., Fontaine, G., & Irwin, M. J. 2000, AJ, 119, 241
Lei, Z., Zhao, J., Németh, P., & Zhao, G. 2019, ApJ, 881, 135
Luo, Y.-P., Németh, P., Liu, C., Deng, L.-C., & Han, Z.-W. 2016, ApJ, 818, 202
Mackebrandt, F., Schuh, S., Silvotti, R., et al. 2020, A&A, 638, A108
McCook, G. P. & Sion, E. M. 1987, ApJS, 65, 603
Miller Bertolami, M. M., Althaus, L. G., Unglaub, K., & Weiss, A. 2008, A&A, 491, 253
Németh, P., Kawka, A., & Vennes, S. 2012, MNRAS, 427, 2180
O'Donoghue, D., Kilkenny, D., Koen, C., et al. 2013, MNRAS, 431, 240
O'Donoghue, D., Koen, C., Lynas-Gray, A. E., Kilkenny, D., & van Wyk, F. 1998, MNRAS, 296, 306
O'Donoghue, D., Lynas-Gray, A. E., Kilkenny, D., Stobie, R. S., & Koen, C. 1997, MNRAS, 285, 657
Oreiro, R., Østensen, R. H., Green, E. M., & Geier, S. 2009, A&A, 496, 827
Østensen, R. H. 2012a, in Astronomical Society of the Pacific Conference Series, Vol. 452, Fifth Meeting on Hot Subdwarf Stars and Related Objects, ed. D. Kilkenny, C. S. Jeffery, & C. Koen, 233
Østensen, R. H. 2012b, in Astronomical Society of the Pacific Conference Series, Vol. 452, Fifth Meeting on Hot Subdwarf Stars and Related Objects, ed. D. Kilkenny, C. S. Jeffery, & C. Koen, 233

Ramsay, G. & Hakala, P. 2005, MNRAS, 360, 314
Ramsay, G., Napiwotzki, R., Hakala, P., & Lehto, H. 2006, MNRAS, 371, 957
Randall, S., van Grootel, V., Fontaine, G., Charpinet, S., & Brassard, P. 2009, A&A, 507, 911
Randall, S. K., Calamida, A., Fontaine, G., Bono, G., & Brassard, P. 2011a, ApJ, 737, L27
Randall, S. K., Calamida, A., Fontaine, G., Bono, G., & Brassard, P. 2011b, ApJ, 737, L27
Randall, S. K., Fontaine, G., Charpinet, S., et al. 2006, ApJ, 648, 637
Randall, S. K., Fontaine, G., Geier, S., Van Grootel, V., & Brassard, P. 2014, A&A, 563, A79
Reed, M., Armbrecht, E., Telting, J., et al. 2018, MNRAS, 474, 5186
Reed, M. D., Kilkenny, D., O'Toole, S., et al. 2012, MNRAS, 421, 181
Reed, M. D., Telting, J. H., Ketzer, L., et al. 2019, MNRAS, 483, 2282
Reed, M. D., Yeager, M., Vos, J., et al. 2020, MNRAS, 492, 5202
Reindl, N., Geier, S., Kupfer, T., et al. 2016, A&A, 587, A101
Rodríguez-López, C., Ulla, A., & Garrido, R. 2007, MNRAS, 379, 1123
Sahoo, S. K., Baran, A. S., Heber, U., et al. 2020b, MNRAS, 495, 2844
Sahoo, S. K., Baran, A. S., Sanjayan, S., & Ostrowski, J. 2020a, MNRAS, 499, 5508
Saio, H. & Jeffery, C. S. 2000, MNRAS, 313, 671
Saio, H. & Jeffery, C. S. 2002, MNRAS, 333, 121
Schuh, S., Huber, J., Dreizler, S., et al. 2006, A&A, 445, L31
Van Grootel, V., Charpinet, S., Fontaine, G., Brassard, P., & Green, E. M. 2014, in Astronomical Society of the Pacific Conference Series, Vol. 481, 6th Meeting on Hot Subdwarf Stars and Related Objects, ed. V. van Grootel, E. Green, G. Fontaine, & S. Charpinet, 115
Vennes, S., Kawka, A., & Németh, P. 2011, MNRAS, 410, 2095
Webbink, R. F. 1984, ApJ, 277, 355
Woudt, P. A., Kilkenny, D., Zietsman, E., et al. 2006, MNRAS, 371, 1497
Zong, W., Charpinet, S., & Vauclair, G. 2016, A&A, 594, A46